Project no. 265863

ACCESS

Arctic Climate Change, Economy and Society

Instrument: Collaborative Project
Thematic Priority: Ocean.2010-1 "Quantification of climate change impacts on economic sectors in the Arctic"

D 2.42 - Calculation of fuel consumption per mile for various ship types and ice conditions in past, present and in future

Due date of deliverable: **31/03/2014**

Actual submission date: 04/09/2014

Used Person/months: **5**

Start date of project: **March 1st, 2011** Duration: **48 months**

Organisation name of lead contractor for this deliverable: **HSVA**

Project co-funded by the European Commission within the Seventh Framework Programme (2007-2013)		
Dissemination Level		
PU	Public	X
PP	Restricted to other programme participants (including the Commission Services)	
RE	Restricted to a group specified by the consortium (including the Commission Services)	
CO	Confidential, only for members of the consortium (including the Commission Services)	

Contents

List of Figures

Abbreviations:

Abbreviation	Long name
HSVA	The Hamburg ship Model Basin
ETA	Estimated Time of Arrival
ARCDEV	Arctic Demonstration and Exploratory Voyage
NSR	Northern Sea Route
NWP	North West Passage
BSFC	Brake Specific Fuel Consumption
Lpp	Length between Perpendiculars
LoA	Length over All
LoW	Length of Waterline
AP	Aft Perpendiculum
FP	Fore Perpendiculum
FPP	Fixed Pitch Propeller
CPP	Controllable Pitch Propeller

1. Introduction

1.1 Background

The past few decades showed a dramatic decline of the Arctic sea ice level, peaking in a record minimum ice extent in 2011. These circumstances generated a high interest in establishing new trade routes, especially in the field of economically viable shipping in arctic regions. Ensuring exploration, access and extraction of resources in this environment will be of great value concerning the prospective trend of offshore engineering and economy.

Even though increasing arctic shipping may provide commercial and social development opportunities the resulting environmental impacts must be investigated intensively.

Several studies have assessed the potential impacts of international shipping on climate and air pollution and have demonstrated that ships contribute significantly to global climate change and health impacts through emission of many pollutants such as carbon dioxide (CO2), methane (CH4), nitrogen oxides (NOx), sulphur oxides (SOx), carbon monoxide (CO), and various species of particulate matter (PM) including organic carbon (OC) and black carbon (BC). Although at present the shipping in Arctic Ocean makes up a relatively small proportion of global shipping emissions, there are region-specific effects from substances such as BC and ozone (O_3) which are becoming increasingly important to quantify and understand.

To better understand the impact of shipping in arctic area, this document focuses on the fuel consumption of different ship types and estimates the exhaust emissions in relation to fuel consumption data.

1.2 Task Description

The routing software, ICEROUTE, will be used to calculate the fuel consumption as a function of power, ice conditions and speed for various ship types traveling on different ice routes in the Arctic. The program uses input data of ice parameters (ice thickness, concentration strength) as well as other environmental data like current and wind speed to calculate the resistance, required thrust and power for a specific ship which is also specified by characteristic data. The result of this simulation is the basis for an exhaust gas emission value calculated from the actual power consumption per mile for each leg and for the total voyage. In addition to the gas emission the discharge of warm engine cooling water can be determined. Calculations will be carried out using existing data from the past (1960 to 2000), the present (2000 to 2010) and ice data as predicted (scenarios). This task is the continuation of ACCESS Task 2.15 with respect to air pollution. The results of the calculation for the past and present periods will be benchmarked against measured values as obtained in 2.41; hereby adjustments will be made to improve the predictions of emission values of future Arctic shipping [1].

1.3 Objectives

The assessment of the aforementioned impact on the environment is carried out by a program. Based on the existing programs ETA (Estimated Time of Arrival),ICEROUTE was developed at HSVA Arctic Technology and extended with new improved modules to the program. The fuel consumption of different types of ship with different propulsion arrangements is to be determined for operation in different ice conditions along the Northern Sea Route (NSR). The determined values for fuel consumption will then be used to predict exhaust emissions depending on consumed power per nautical mile.
The advance code shall then be used to carry out calculations for different arctic routes. The calculation is based on data for ice conditions in the period of 1960-2040, within the period of April to November.

Four different transit routes along the Northern Sea Route are considered. All routes start from Murmansk and lead to Bering Strait via different alternatives that are further specified in section 3. Several different ship types are calculated:

- Bulk carrier,

- Oil tanker,

- LNG carrier.

2. Description of HSVA Program Ice Route with Extended Module for the Calculation of Fuel Consumption and Exhaust Emissions

2.1 General description

The programs ETA and ICEROUTE have been developed at HSVA within the research project ARCDEV in 1998 [2] and is based on semi empirical - analytical formulations for predicting ship resistance in different environmental conditions including ice coverage. Additionally the data of the specific propulsion arrangement are used to calculate the required power and thereby obtain the maximum attainable speed. The routes are subdivided into legs while the number of legs is chosen according to the required spatial resolution with regard to variations in environmental conditions. In a second step the traveling time for the entire route can be determined by summation of travel time for each leg. In a third step with the information of the specific engine data the fuel consumption can be determined. And finally the exhaust emissions are calculated by defining emission factors for the consumed fuel [3]. The calculation steps and required data are shown in Figure 1 and

Figure **2**.

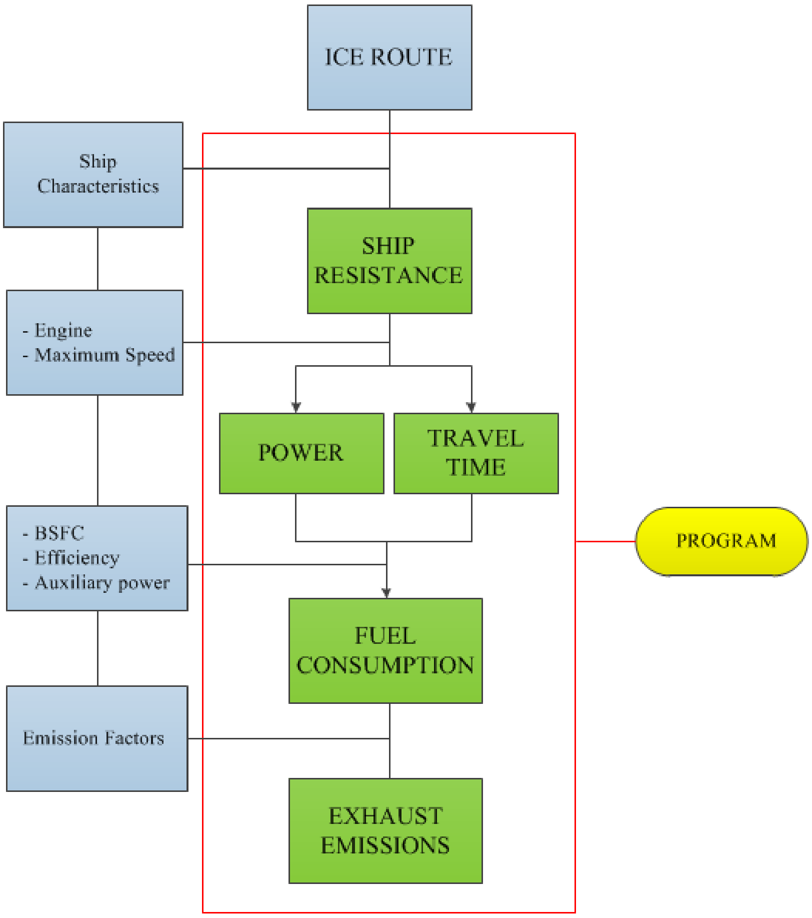

Figure 1 Flow Chart of the calculation process

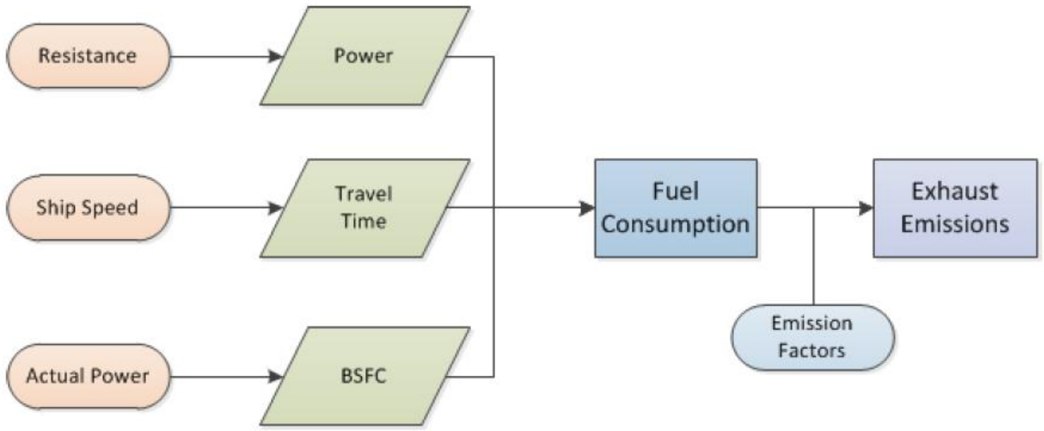

Figure 2 Calculation of fuel consumption and exhaust emissions

As we already chose three kinds of ships to calculate, i.e. bulk carrier, oil tanker and LNG carrier, for each ship type many available configurations can be considered. For example, with regard to the propeller type, a ship can be equipped with either a controllable pitch propeller, a fixed pitch propeller or with a more advanced podded azipod propeller. Considering the engine type, the most common type would be a diesel engine fuelled with heavy fuel oil, but nowadays to fulfil the strict regulations on exhaust gases in sensitive regions (Emission Control Areas), vessels are sometimes equipped with new kinds of engines such as dual fuel. And it is also necessary to mention that for the LNG carrier, steam engine is still a very common type of engine that can be seen in many vessels even for some new building ships of our time.
Since it is not possible to consider all the available alternatives which a ship owner can choose to use with a vessel, the study can be carried out with the subsequently shown configurations.

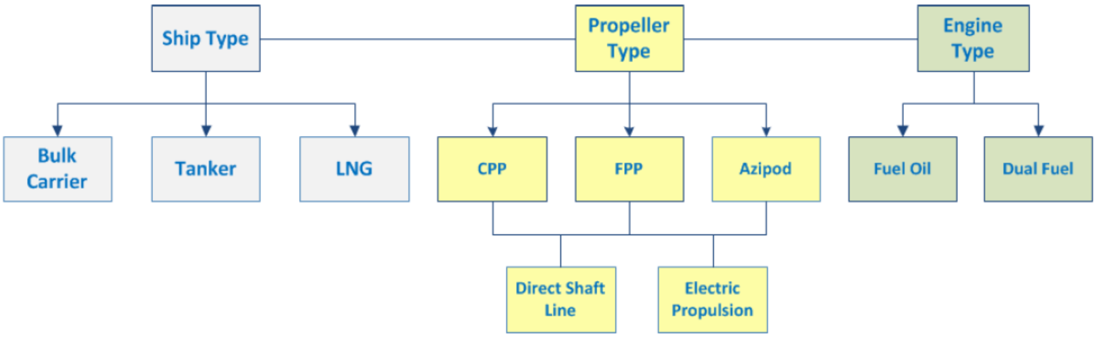

Figure 3 Different Vessel Configurations

The calculations aiming on the ice performance and travel time prediction are explained in ACCESS report D 2.16 [4]. Additional extensions are explained in the following sections.

2.2 Fuel Consumption of Ships in Ice Conditions

The increase in resistance resulting from ice navigation leads to higher fuel consumption rates for the vessels. In addition, delays due to ice may lead to a longer duration of the voyage which in turn also leads to more total fuel consumption. The fuel consumption rate of a vessel depends on a variety of factors, such as the vessel type itself, the environmental conditions the vessel is facing, and the vessel's operating scenarios. Vessels are designed based on estimated resistance values and built with engines which have established specific fuel consumption values. Old vessels usually have less fuel efficiency than new ones due to hull degradation, engine performance deterioration and recent efficiency based technological improvements in vessel and engine design.

The environmental conditions which ships operate in affect the vessel's total resistance and consequently the fuel consumption rate. Vessels operating in head seas, strong wind and ice conditions experience more resistance and consequently burn more fuel than vessels operating in calm seas and sheltered waters. The vessel's operating scenario and schedule such as speed, heading, routing, manoeuvres, and the use of auxiliary systems, affects the overall fuel consumption.

In order to investigate the fuel consumption profile for a vessel a number of different methods can be utilized, such as numerical calculation and prediction of fuel consumption and demand, actual field measurements of fuel consumption rates or simply considering fuel expenses per trip, per person or per year.

2.2.1 Brake Specific Fuel Consumption (BSFC)

BSFC is a measure of fuel efficiency within a shaft reciprocating engine [5]. It may also be thought as power-specific fuel consumption, for this reason. BSFC is a possibility to directly compare the fuel efficiency of different reciprocating engines. In the following equation the rate of fuel consumption is divided by the power produced.

$$\mathrm{BSCF} = \frac{\mathrm{r}}{\mathrm{P}} \qquad (1)$$

Whereas the fuel consumption rate *r* is measured in grams per second [g/s] or kilograms per hour [kg/h]. *P* is the power produced in watts [W] or in kilowatts [kW] and can be described by the product of the engine torque *T* in newton meters [Nm] and ω , the engine speed in radians per second [rad/s].

The resulting units of BSFC are grams per joule [g/J] or grams per kilowatts-hour [g/kWh].

The actual efficiency of an engine depends on the fuel being used. The energy densities of different fuels are defined by the fuel's heating values. The lower heating value (LHV) is used for internal combustion engine efficiency calculations because the heat at temperatures below 150°C cannot be put to use.

There are many other factors that influence the mass fuel consumption of a vessel. For instance, in Figure 4 an average data set analysed from over 600 measured cases of a container ship at sea is presented. This average line can be used to correct the BSFC and relates to the actual power of the vessel, as shown in Figure 5.

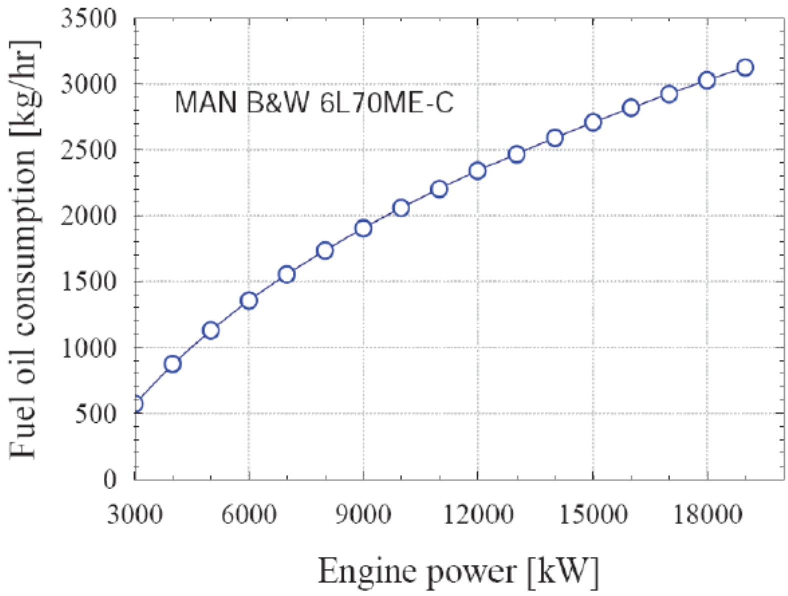

Figure 4 Fuel consumption measured on a ship at different power levels **[6]**

Practically, we use this correlation between the BSFC and the actual power when we calculate the fuel consumption of all ships. The correlation can be expressed in form of the following equation:

$$\Delta\mathrm{BSFC} = 6610.6\,x^6 - 20524\,x^5 + 23791\,x^4 - 11985\,x^3 + 1803.2\,x^2 + 340.12\,x - 36.733 \quad (2)$$

Here $x = P/P_{MCR}$ denotes the ratio of actual power and the maximum continuous rate power. The variation Δ *BSFC* is added to the standard value which is usually available in every technical document from engine manufacturers.
The fuel consumption is then calculated by the equation:

$$\mathrm{FC} = \mathrm{BSFC} \cdot \mathrm{P} \quad (3)$$

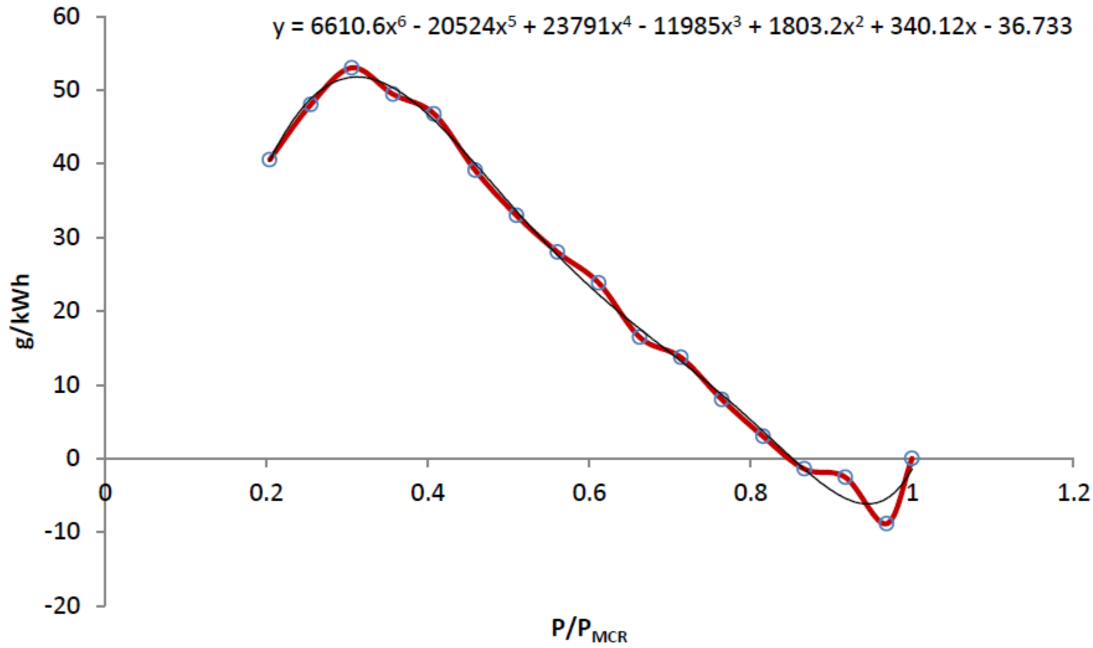

Figure 5 Variation of BSFC corrected from actual fuel consumption **[3]**

2.3 Exhaust emissions from ships

Since 1990s, IMO, EU, and the EPA came up with the Tier I exhaust gas emission norms for the existing engine in order to reduce nitrogen oxides and sulphur oxides. Harsher Tier II and Tier III were later announced for newer engines. Figure 6 shows different levels of requirements for the NOx emission according to three different Tiers.

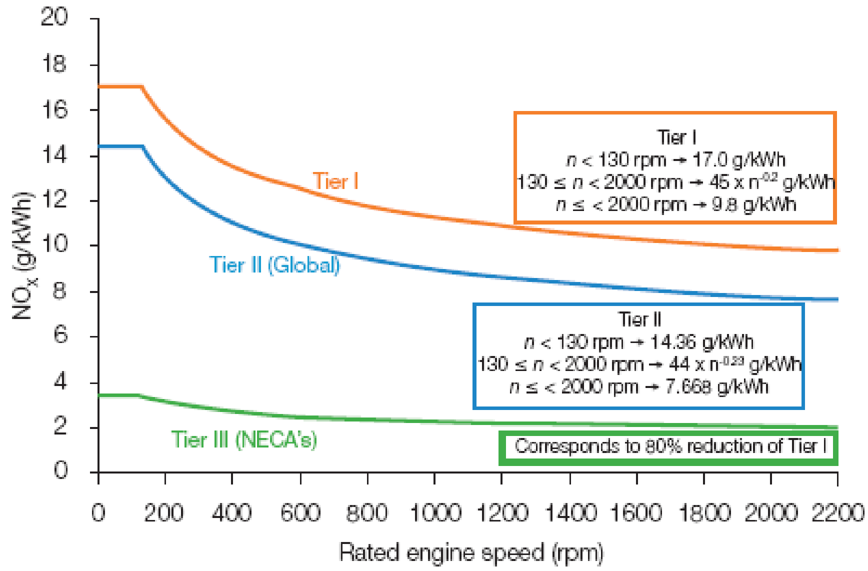

Figure 6 IMO NO_X Limitations **[7]**

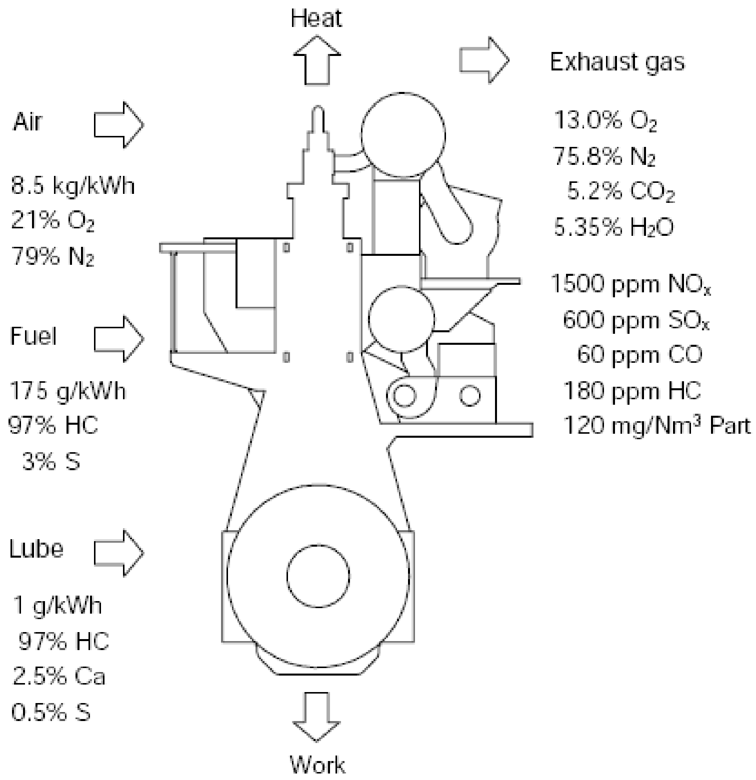

Figure 7 Typical Emission components from a low-speed diesel engine **[8]**

Diesel fuels commonly used in marine engines are a form of residual fuel, also known as dregs or heavy fuel oil (HFO). They are cheaper than marine distillate fuels but contain higher amount of nitrogen, sulphur and ash content. This significantly increases the NOx and SOx in the exhaust gas emission. The diesel engine combustion process almost always leaves by-products of oxides of nitrogen, unburned hydrocarbons, carbon monoxides and particulate matter.

Nitrogen oxides are a group of toxic gases formed by the reaction of nitrogen and oxygen. At extremely high temperature of combustion, these two gases react to nitrogen dioxide NO_2, and nitrogen oxide NO. These gases are major source of ground level ozone and are also a significant source of acid rains and soot formation.

Unburned hydrocarbons come from unburned or partially burned fuel after combustion process. These hydrocarbons are toxic in nature, having adverse effects on our health and in some cases are known to cause cancer.

Carbon monoxide is formed as an intermediate product of hydrocarbons fuel combustion due to the lack of adequate oxygen to form carbon dioxide or due to insufficiently high temperature.

2.4 Assessment of emissions

One possibility to calculate emissions of a ship using emission factors is described by the following formula.

$$E_{ijk} = EF_{ij} \cdot LF_{jk} \cdot \frac{KW_j}{\eta_j} \cdot T_{jk} \quad (4)$$

- E_{ijk} are emissions of type *i* from vessel *j* on route *k* in gram [g]
- EF_{ij} is the emissions factor for emissions of type *i* on vessel *j* in [g/kWh]
- LF_{jk} is the average engine load factor for vessel *j* on route *k* and takes into account periods of manoeuvring, slow cruise, and full cruise operations;
- KW_j is the rated main engine power in kilowatts [kW] for vessel *j,*
  η_j is the engine efficiency
- T_{jk} is the duration of the trip for vessel *j* on route *k* in hour [h]

In Table 1 we can find the emission factors that are applied to the emissions from ships in Arctic area at the present and in the future. Emissions depend on different types of engines, with various speeds of revolutions, range of power and different fuels used.

Table 1 Gas and particulate matter emission factors applied to current and future Arctic shipping [g/kg] **[8]**

Pollutant	Ship type	2004	2020	2030	2050
CO	All	7.4	7.4	7.4	7.4
NOx	Transport	78	67	56	56
	Fishing vessel	56	56	56	56
PM	Transport	5.3	1.4	1.4	1.4
	Fishing vessel	1.1	1.1	1.1	1.1
SOx	Transport	54	10	10	10
	Fishing vessel	10	10	10	10
CO2	Transport	3206	3206	3206	3206
	Fishing vessel	3114	3114	3114	3114
BC	All	0.35	0.35	0.35	0.35
OC	All	1.07	0.39	0.39	0.39

2.5 Fixed and controllable pitch propeller

In these calculations the effects of using a fixed pitch propeller (FPP) will be compared to sailing with a controllable pitch propeller (CPP). Therefore this short introduction points out the major differences between the two concepts.

Figure 8 shows the correlation of a ship speed in different ice concentrations. It furthermore states a curve of a safe speed for ships in ice. As the speed of a ship in ice is limited due to higher resistance compared to open water resistance, it is necessary to further specify a safe speed in order to avoid damaging of the hull by collision with ice features. At low concentrations a ship is able to push ice and floes aside with a relatively high speed, whereas at higher concentrations, the resistance increases and forces the ship to travel slower. The safe speed curve does not state the maximum attainable velocities in ice conditions. Thus a ship travelling at a low concentration might reach a maximum speed ahead above safe speed, which would result in a higher fuel consumption compared to safe speed.

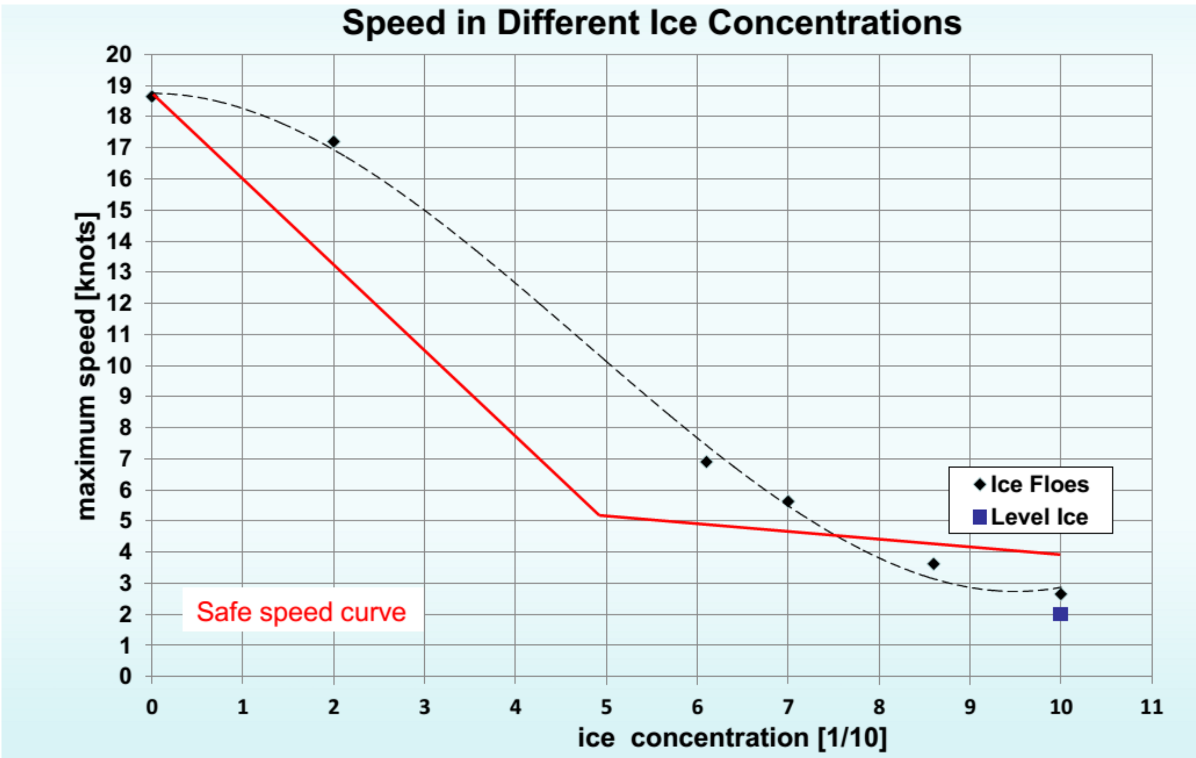

Figure 8 Speed of ship depending on ice concentration

FPP

The fixed pitch propeller is commonly optimized for a single specific speed of a ship which usually is the design condition in calm water with a small margin for heavier sea states. Thus the FPP is over-pitched or under-pitched for certain other operation conditions. In ice the ship usually operates at lower speeds but at the same time has to provide high thrust to overcome the additional resistance. Therefore the propeller curve (required rotational power at propeller vs. propeller rate) is rising faster and hits the engine limit curve at lower rates (Figure 9). Therefore the actual power which can be delivered by the engine is significantly lower than the installed engine power and the corresponding attainable speed of the ship is limited.

CPP

A controllable pitch propeller is a propeller arrangement that can adjust the blades pitch along their longitudinal axis. It allows a vessel a more efficient manoeuvring (e.g. stopping) compared to an FPP arrangement, as it does not adjust the rate of turning or even turning direction of the drive shaft but the pitch of the blades to produce stern thrust.

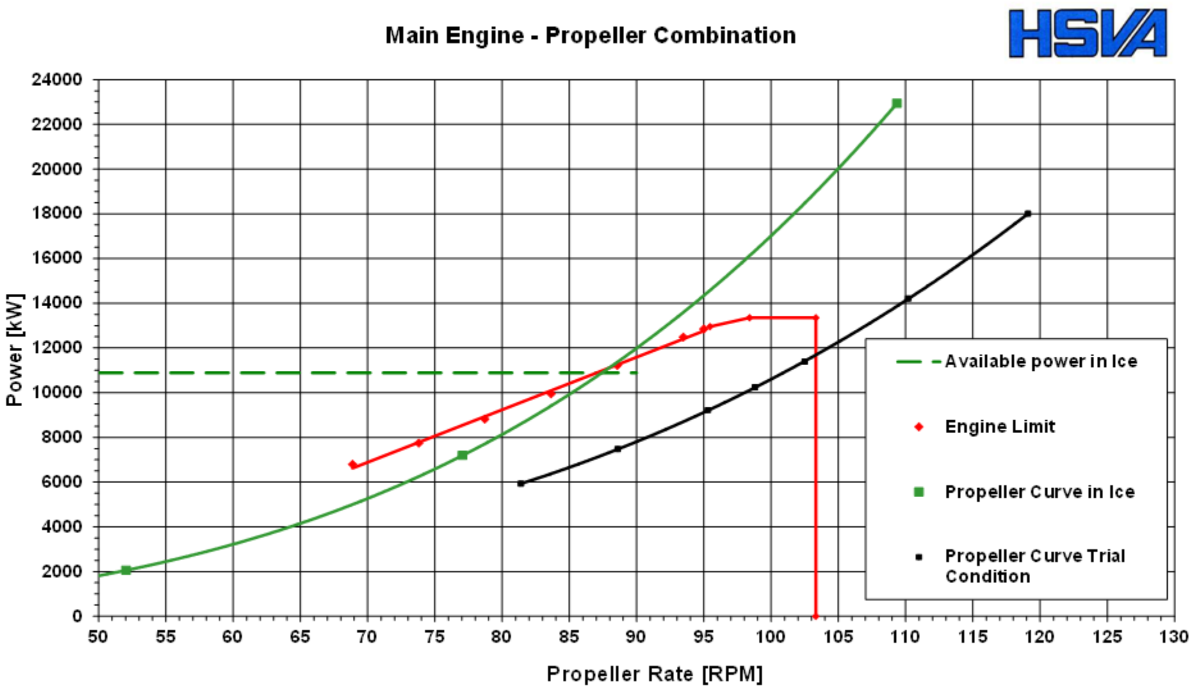

Figure 9 Power over turning rate with engine limit (FPP)

In Figure 9 a characteristic curve of a motor is shown in combination with the propeller curve in ice and trial condition. As resistance increases, the required torque to deliver enough power rises with the decreasing propeller rate. The black curve shows the trial condition, while in operating state the resistance grows due to sea state, wind, fouling or in this case due to ice. This results in lower propeller rates and consequently lower engine output. A CPP is a possibility to react to these circumstances. Likewise a CPP is much more complex and thus more expensive than a FPP, but in return concerning the single optimized velocity, not more efficient.

3. Investigated Scenarios

3.1 Investigated Ships

The following section states the main data sheets of the seven vessels investigated.

3.1.1. Bulker

Table 2 Main data sheet Bulker

Type of Ship	Bulker	Amount of Propeller	1
Ship size/Class	Panamax	Diameter (m)	6.50
Built	2012	Type	Conventional CPP
Ice class	DNV ICE-1A	Power (kW)	11620
Displacement (tons)	68416	Builder	KaMeWa
DWT (tons)	56327	Bow and stern thrusters	(2x) 800 kW
Loa (m)	197.07	Main engine	MAN B&W 7S50MC-C8.1-TII
Lpp (m)	189.00	RPM	127
Lwl (m)	194.84	Main engine ouput (kW)	11620
Breadth moulded (m)	32.26	Fuel grade	IFO380
Draft (m)	11.1	SFOC (g/kWh)	175
Depth moulded (m)	18.5	Auxiliary Power (kW)	2880
Speed open water (knots)	15.5		
Save speed in ice (knots)	8.0		

3.1.2 Tanker01

Table 3 Main data sheet Tanker01

Type of Ship	Oil Tanker	Amount of Propeller	2
Ship size/Class	Panamax	Diameter (m)	6.00
Built	2009	Type	ABB Azipod V23
Ice class	LU6 (eq. IA Super)	Power (kW)	17000 (together)
Displacement (tons)	102,000	Builder	ABB
DWT (tons)	70,000	Bow and stern thrusters	2000 kW
Loa (m)	257.00	Main engine	(4x) Wärtsilä 9L38 6525kW
Lpp (m)	236.00	RPM	600
Lwl (m)	243.30	Main engine ouput (kW)	26100
Breadth moulded (m)	31.00	Fuel grade	IFO 380
Draft (m)	14	SFOC (g/kWh)	177
Depth moulded (m)	20.8	Auxiliary Power (kW)	-
Speed open water (knots)	16.0		
Save speed in ice (knots)	8.0		

3.1.3 Tanker02

As the Tanker02 is equipped with a controllable pitch propeller (CPP) there will be several scenarios investigated to assess the effect of the adjustment of CPPs. The program is not capable of adjusting the pitch during a calculation for a transit. So there will be three ships simulated with particular angles of pitch to cover three cases and thus the adjustment of a CPP. The pitch adjustment for the three different models is as follows: Tanker 021: 0.624 ; Tanker 022: 0.790; Tanker 023: 0.877.

Table 4 Main data sheet Tanker02

Type of Ship	Oil Tanker	Amount of Propeller	1
Ship size/Class	Panamax	Diameter (m)	6.50
Built	2007	Type	Conventional CPP
Ice class	DNV ICE-1A	Power (kW)	13560
Displacement (tons)	81400	Builder	Rolls-Royce
DWT (tons)	74999	Bow and stern thrusters	-
Loa (m)	228.50	Main engine	MAN 6S60MC-C7.1-TII
Lpp (m)	220.00	RPM	105
Lwl (m)	226.80	Main engine ouput (kW)	13560
Breadth moulded (m)	32.24	Fuel grade	IFO380
Draft (m)	14.7	SFOC (g/kWh)	174
Depth moulded (m)	20.45	Auxiliary Power (kW)	2730
Speed open water (knots)	15.1		
Save speed in ice (knots)	6.0		

3.1.4 LNG Carrier (l/h)

For the calculation of the LNG Carrier two ships will be investigated. The first ship delivers a low and the second one a higher power for the propeller.

Table 5 Main data sheet LNG Carrier

Type of Ship	LNG Carrier	Amount of Propeller	3
		Diameter (m)	6.0
Built	2010	Type	Electric propulsion
Ice class	DNV ICE-1A	Power (kW)	27,300(l)/ 41000 (h)
Displacement (tons)	115,500	Builder	MMG
Tank Capacity (m^3)	173,400	Bow and stern thrusters	-
Loa (m)	290.00	Main engine	(3x) Wärtsilä 12V50 DF + 9L50 DF
Lpp (m)	279.00	RPM	610 (78)
Lwl (m)	287.63	Main engine ouput (kW)	42,000
Breadth moulded (m)	45.80	Fuel grade	DF
Draft (m)	11.95	SFOC (g/kWh)	175
Depth moulded (m)	26.50	Auxiliary Power (kW)	-
Speed open water (knots)	19.5		
Save speed in ice (knots)	7.0		

Table 6 Assessment of emission factors

Pollutant	Tanker01	Tanker02	Bulker	LNG Carrier	Unit
CO2	3480.00	3206.00	3206.00	2543.00	[g/kg fuel]
NOx	54.90	78.00	78.00	54.86	[g/kg fuel]
SOx	22.80	54.00	54.00	0.00	[g/kg fuel]
CO	2.85	7.40	7.40	7.43	[g/kg fuel]
BC	0.35	0.35	0.35	0.35	[g/kg fuel]
OC	1.07	1.07	1.07	1.07	[g/kg fuel]
PM	2.29	5.30	5.30	0.57	[g/kg fuel]

Table 6 lists the assumed factors taken into account for the calculation of emission [9], directly depending on the fuel consumption. As the Tanker 02 and the Bulk carrier drive similar two-stroke engines, they were assumed to have the same factors for emissions.

3.2 Investigated Routes

The Northern Sea Route is a shipping lane officially defined by russian government from the Atlantic Ocean to the Pacific Ocean specifically running along the Russian Arctic coast from Murmansk on the Barents Sea, along Siberia, to the Bering Strait and Far East. The entire route leads through Arctic waters. Several parts are ice-free for two months per year. At the western end of the NSR, routes from Murmansk across the Barents Sea and Kara Sea, and up the Yenissey River to Dudinka have been taken regularly since the 1980ies, but were not used by commercial transits until 2009.

The NSR is running through Kara, Laptev, East Siberian, and Chukchi seas. Entering the NSR is possible from western directions through the straits Yugorskiy Shar and Karskiye Vorota, or by passing north of Ostrova Novaya Zemlya around Cape Zhelaniya, and from east through the Bering Strait. Regardless of explicit routing, the NSR extends to about 3000 nautical miles. The factual length of the route in each particular case depends on ice conditions and on the choice of variants of passage resulting in individual leg-lengths.

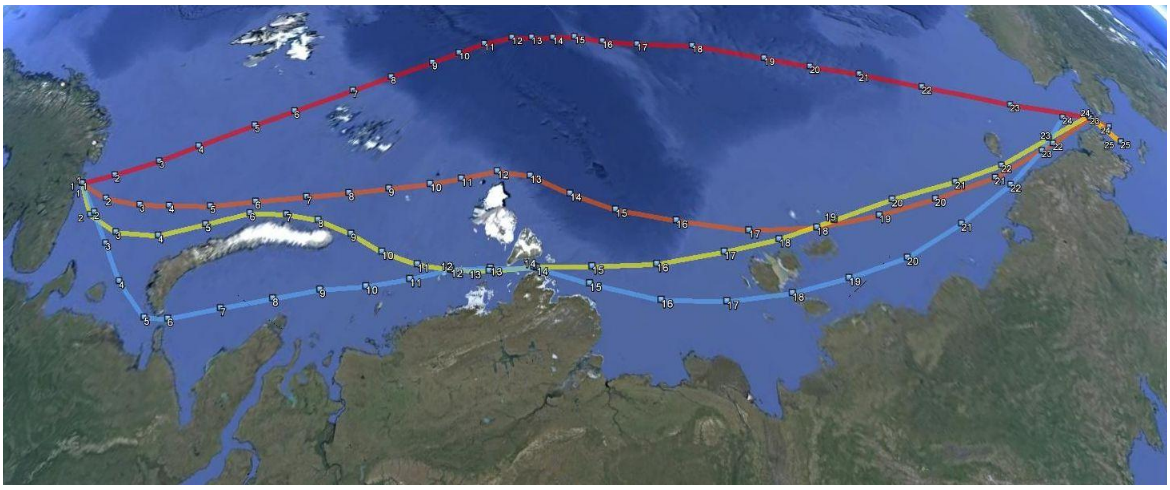

Figure 10 Different transit routes along the NSR: 1 (blue), 2 (yellow), 3 (orange) and 4 (red)

The investigated route profiles can be described by the following approximate waypoints:

Route 1 (blue, 3048 nm) - Murmansk to Bering Strait via Kara gate, south of Severnaya Zemlya and south of New Siberian Islands,

Route 2 (yellow, 2998 nm) - Murmansk to Bering Strait via north of Novaya Zemlya, south of Severnaya Zemlya and north of New Siberian Islands,

Route 3 (orange, 2892 nm) - Murmansk to Bering Strait via north of Novaya Zemlya, north of Severnaya Zemlya and north of New Siberian Islands,

Route 4 (red, 2729 nm) - Murmansk to Bering Strait via north of Novaya Zemlya, north of Severnaya Zemlya close to the geographical north pole and north of New Siberian Islands.

Obviously, the calculation can be carried out for east- and westward transits.

3.3 Investigated Ice Conditions in the Past, Present and Future

The main factor influencing navigation through the NSR is the presence of ice. The navigation season for transit passages on the NSR starts approximately at the beginning of July and lasts through to the second half of November. There are no specific dates for commencement and completion of navigation as it depends on the particular ice conditions. In 2011 the navigation season on the NSR seaways for large vessels constituted 141 days in total, i.e. more than 4.5 months. The data set used in the following figures is provided by the WCRP working group. For the scenarios ice data of the coupled global climate model MPI-ESM-LR [10] part of the World Climate Research Programme (WCRP) Intercomparison Phase 5 (CMIP 5) [11] provided and reviewed by partners from work package 1 [12] were used. The data had been obtained within the framework of the World Climate Research Program and are based on historical scenarios and different emission scenarios for the future defined by emmitted greenhouse gases in the year 2100. For the current investigation the two scenarios rcp 4.5 and 8.5 [13] were used.

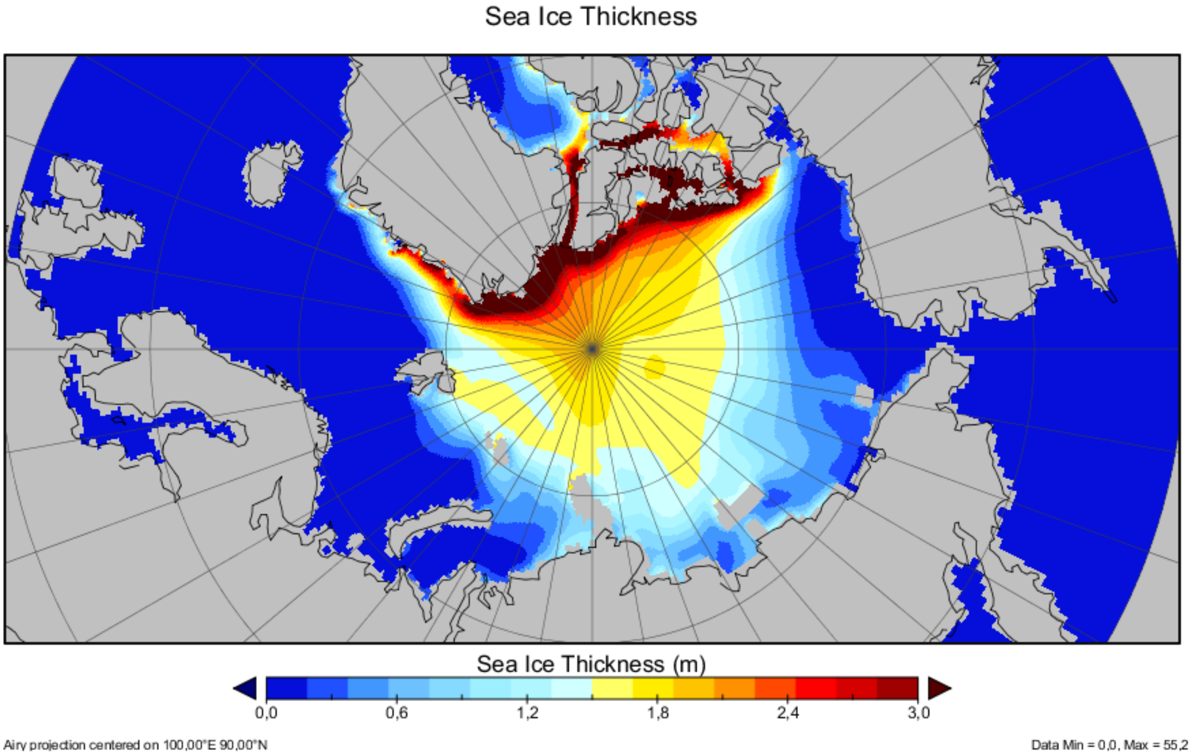

Figure 11 Sea ice thickness data for September 2013 [10]

In recent years quite easier ice conditions have been observed which offers more considerable opportunities for operation at the NSR seaways. Currently all NSR seaways are currently located in ice regimes with one-year ice. In addition to these routes, one route is analysed which leads across the north-pole to survey future ice conditions. In the Arctic conditions first-year ice grows approximately up to 1.6 metres. In early July, at the beginning of the navigation season ice is not pressurized. The ice is broken and can be easily moved through. In September and October the NSR seaways can be completely ice-free. Therefore, the vessel may have the same speed as in open water condition. A voyage from Cape Zhelaniya in Novaya Zemlya to the Bering Strait can be travelled at the speed of 14 knots within 8 days.

The aforementioned decline of sea ice is clearly visible in Figure 11. Even in the pole region the ice thickness does not exceed 2 m. All the routes 1 to 4 navigate through ice conditions from 0,8 m to 1,8 m in thickness (c.f. Figure 10). The data indicates that in September the routes 1 and 2 thick ice layers will not be present and especially with young first-year ice layers. As route 3 passes north of Severnaya Zemlya ice thicknesses of 1,8 m can occur. In this scenario, similar applies to route 4. Figure 12 shows the ice concentration for September 2013 on a range between 0 and 100 per cent. The picture underlines the periodic occurring ice-free conditions for route 1 and 2 in the present and thus in the future decades. In the pole region it shows a high coverage with ice up to 100 per cent.

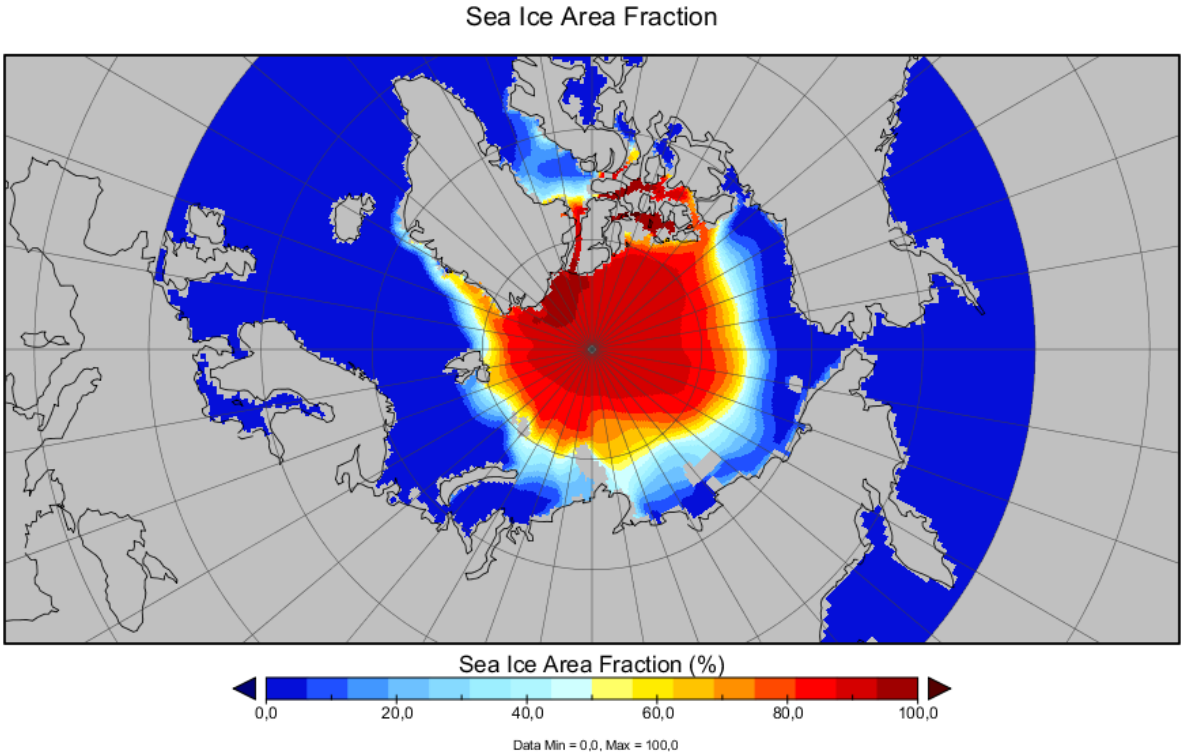

Figure 12 Sea ice concentration data for September 2013 [10]

Figure 13 illustrates variation of sea ice concentration on the NSR. The bulk shown in the first picture shifts up to the pole region and exposes the sea routes used for the calculations. The whole profile scales down to two thirds in total area. The forecasts show a thinning out in future decades to critical lowest values about 50 per cent in 2040, presented in the last picture of Figure 13.

Figure 16 illustrates variation of sea ice thickness on the NSR. Observing from 1960 on a comparatively vast area is covered by thick ice with values above 3 m. This former core area decimated and thinned out. It relocated the core areas to north-american shore, where the ice thickness stays above 3 m, even in the forecasts for future decades. In the northern region of the Kara Sea and the East Siberian Sea the thickness stagnates in coastal waters.

Figure 16 lists ice thickness changes during 80 years including a forecast. Figure 14 shows the variation of ice thickness during the year 2000. Periods are chosen as investigated in the route calculations. The enormous differences become visible by comparing the first and the third picture of Figure 14, whereas in April the whole NSR area is covered with ice. North of the New Siberian Islands the ice thickness becomes up to above 3 m. The area thins out in September and October and frees the routes from ice. Especially for route 1 this resembles open water conditions. As shown in Figure 10, transit routes 2 and 3 pass the New Siberian Islands very close and are confronted with ice all year through.

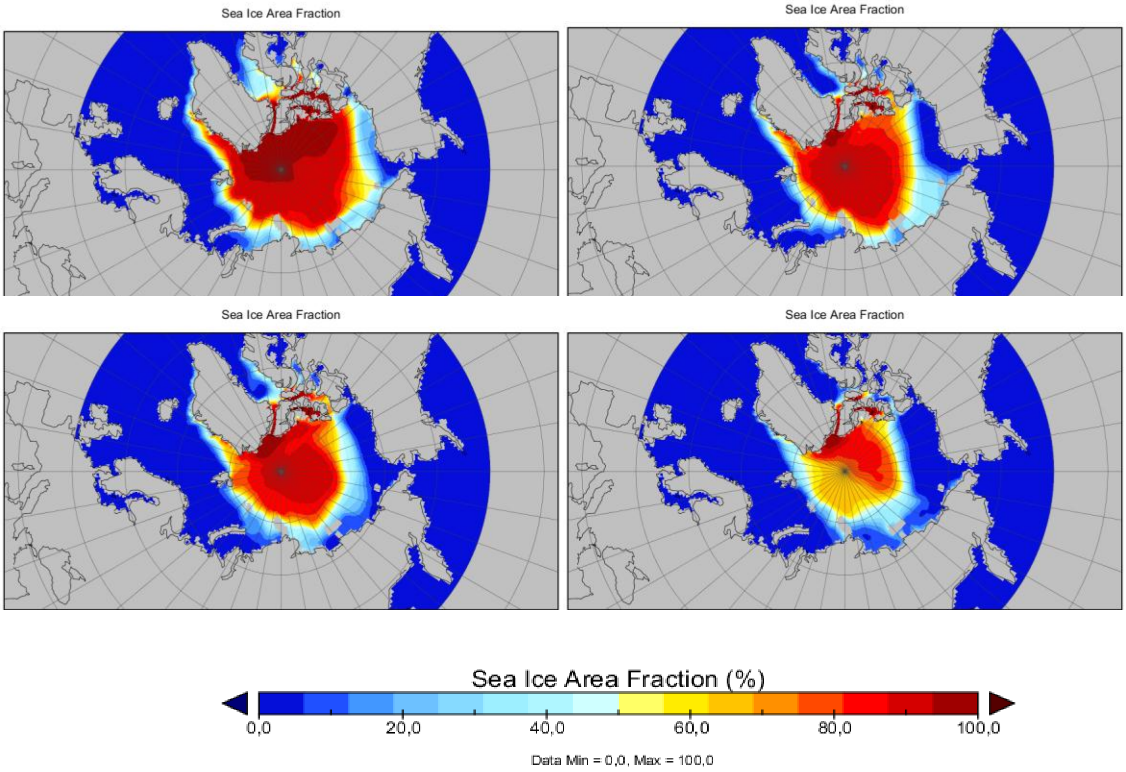

Figure 13 Ice concentration data from September 1960, 2000, 2020 and 2040 [10]

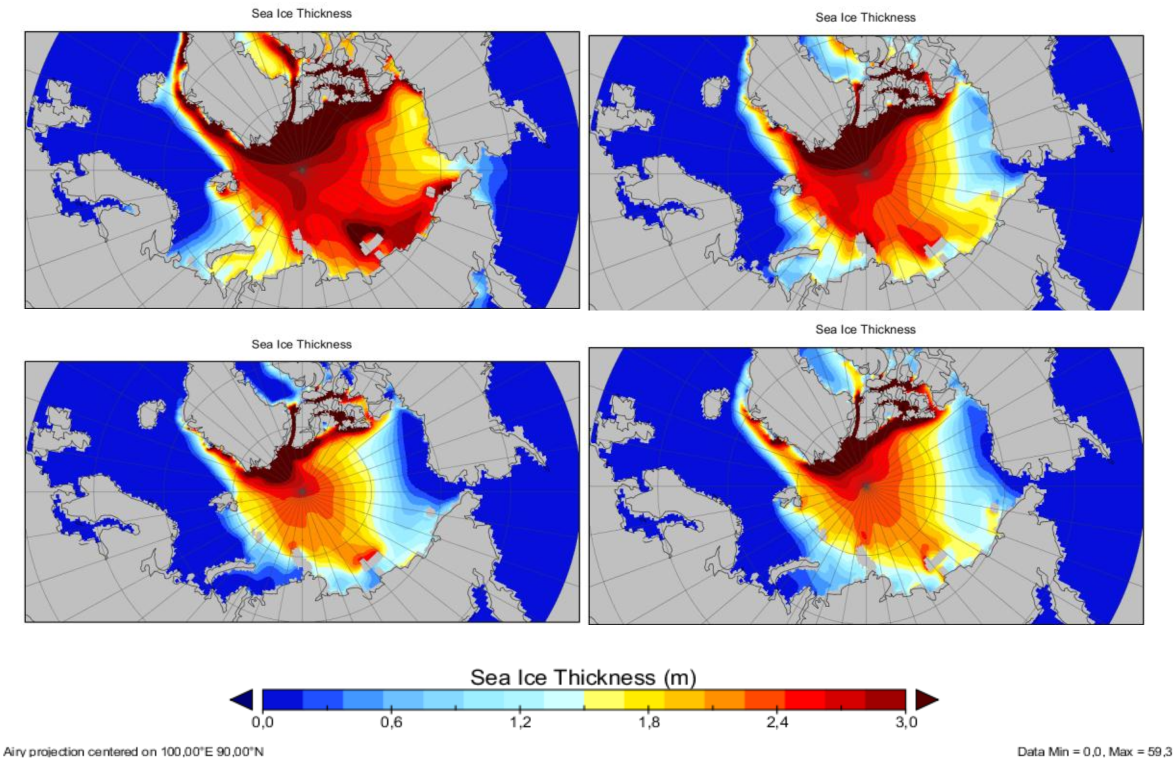

Figure 14 Variance of ice thickness during April, July, September and November 2000 [10]

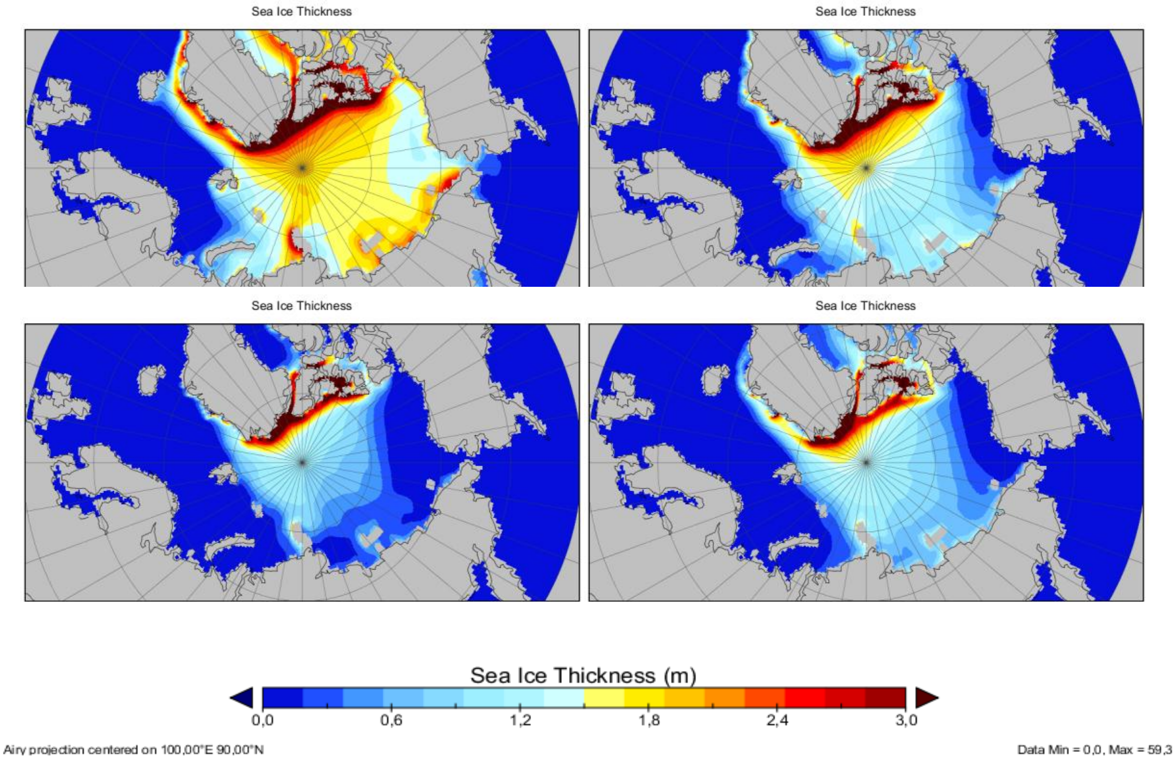

Figure 15 Variance forecast of ice thickness during April, July, September and November 2040 [10]

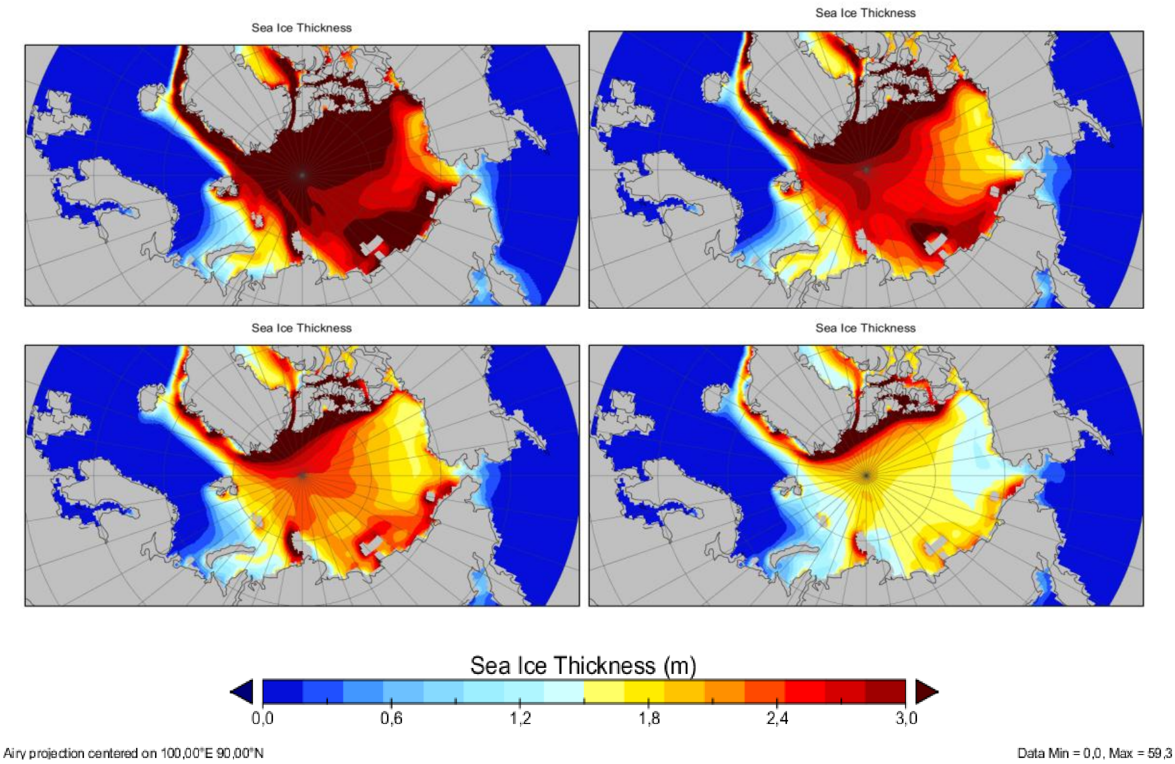

Figure 16 Ice thickness data from April 1960, 2000, 2020 and 2040 [10]

4. Presentation of Results

In section 4.1 the travelling time and fuel consumption calculations are presented. In the next chapter 4.2, the results of the calculations of exhaust gas emissions will be explained.

4.1 Travelling time and fuel consumption

The following bar charts show the results for one ship within a period from 1960 to 2040, including the months April (04), July (07), September (09) and November (11), evaluated on the aforementioned routes 1 to 4. Several bar charts will be shown in each case. The first stated charts provide an overview of all calculated routes. No bar indicates excessing a time threshold of 50 days, which implies every route with a travel time over 50 days is assessed as not completed. The second charts only state completed transits during the whole period taken into account.

Tanker01

The first investigated ship is Tanker01. The results are presented in Figure 17 and Figure 18.

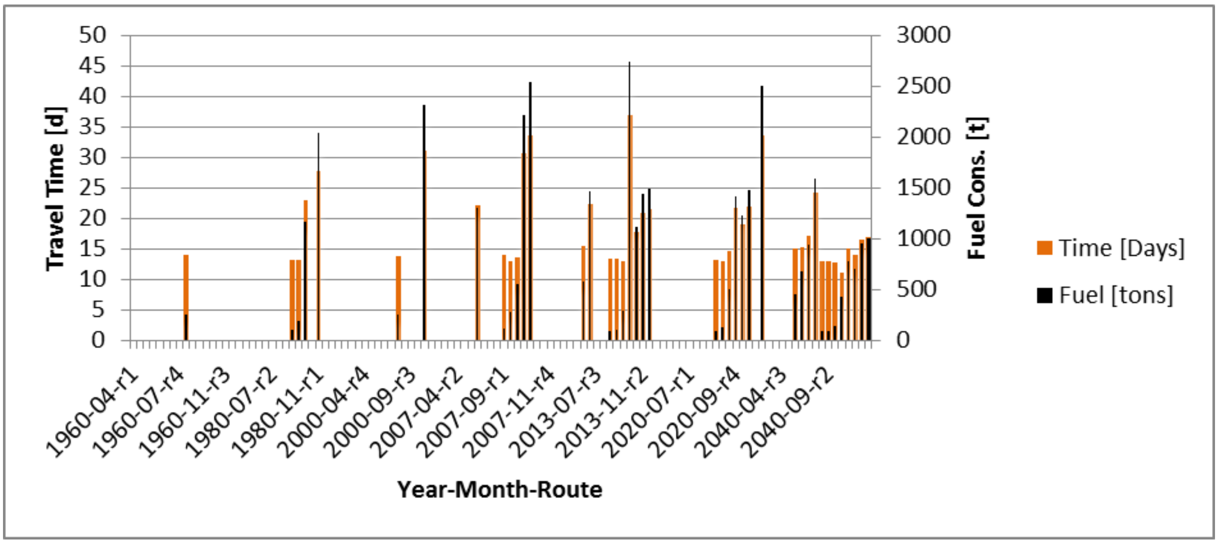

Figure 17 Tanker01 at all calculated routes

The ship shows, according to these calculations, a stable ability to pass the routes 1 to 4, whereas routes 1 and 2 are represented the most. Over the reviewed months, the travel times stays moderate with exceptions on routes 3 and 4 respectively the months November and July. There are no completed transits registered for the month of April. The behaviour of the fuel consumptions resembles the peaking of travelling times.

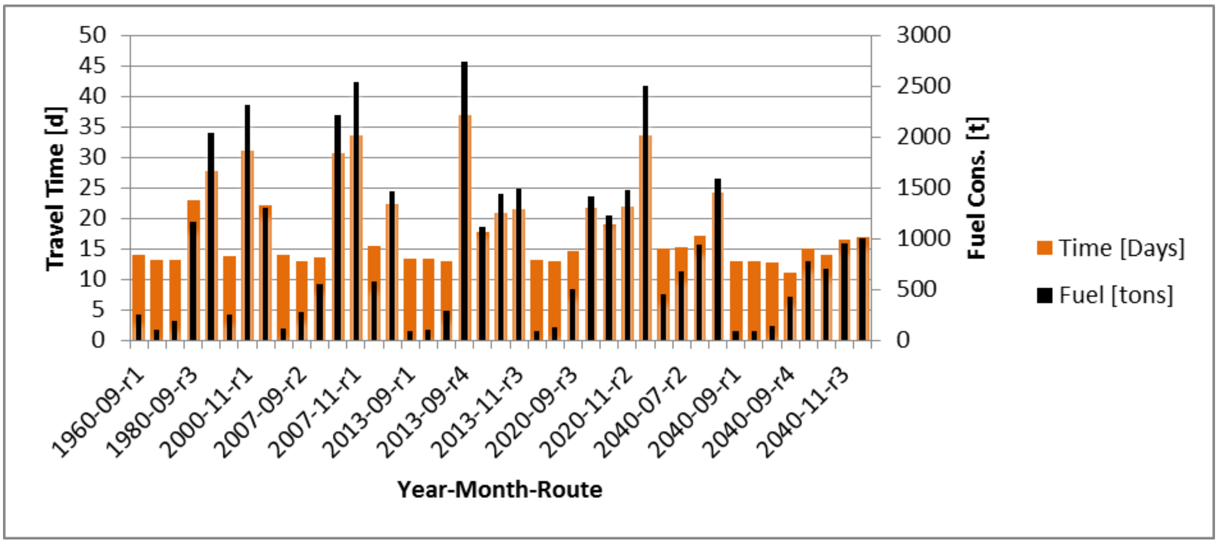

Figure 18 Tanker01, stating only completed transits

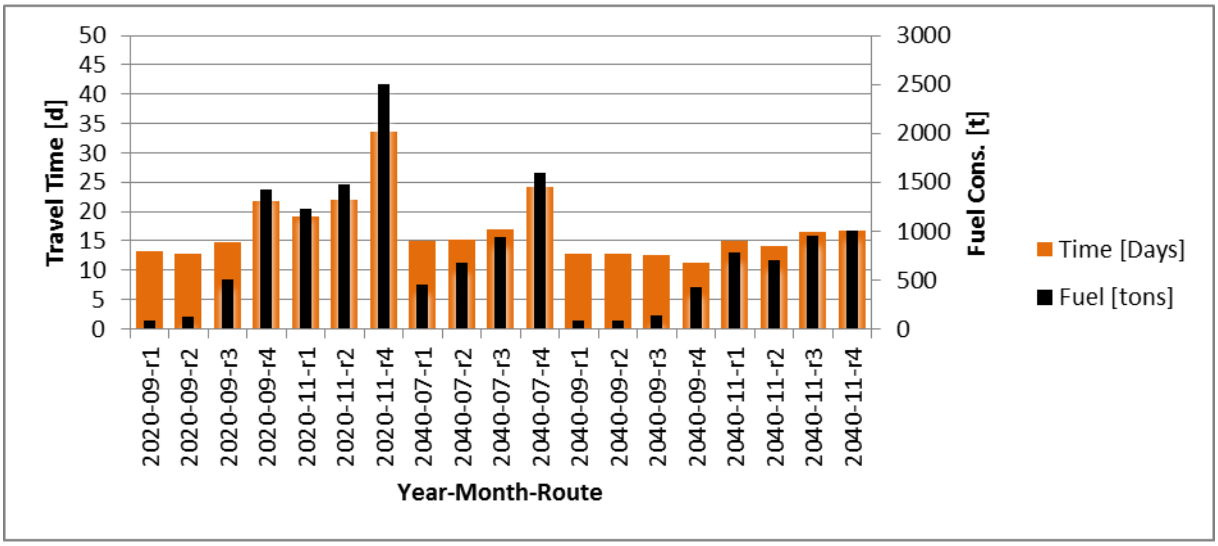

Figure 19 Tanker01, focus on years 2020 and 2040

The focus on the upcoming years coincides with the decline of sea ice level as the routes 1 to 4 will be passable. Clearly visible in Figure 19 the fuel consumption rises with expanding on the pole region route 4. Next to that it is obvious, that the fuel consumptions for about the same traveling time vary. The reason for that is the save speed of the ship. In areas with a small ice coverage the ship is only allowed to sail at a speed where the contact with ice floes may not harm the ship significantly. Thereby it only uses a small percentage of the main engine power. When the ice coverage and thickness is increased the engine operates at higher loads and uses more fuel.

Tanker02

Three cases were investigated for the Tanker02. These cases differ in the propulsion‘s pitch adjustments concerning the CPP. This is the reason why they can be dealt with as one ship.

Tanker021

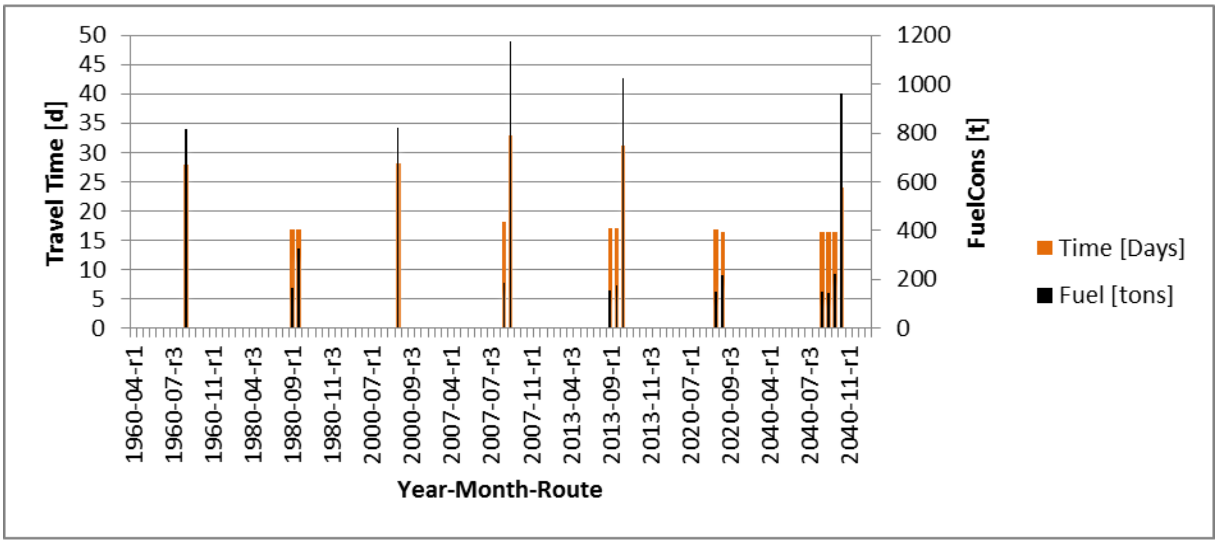

Figure 20 Tanker021 at all calculated routes

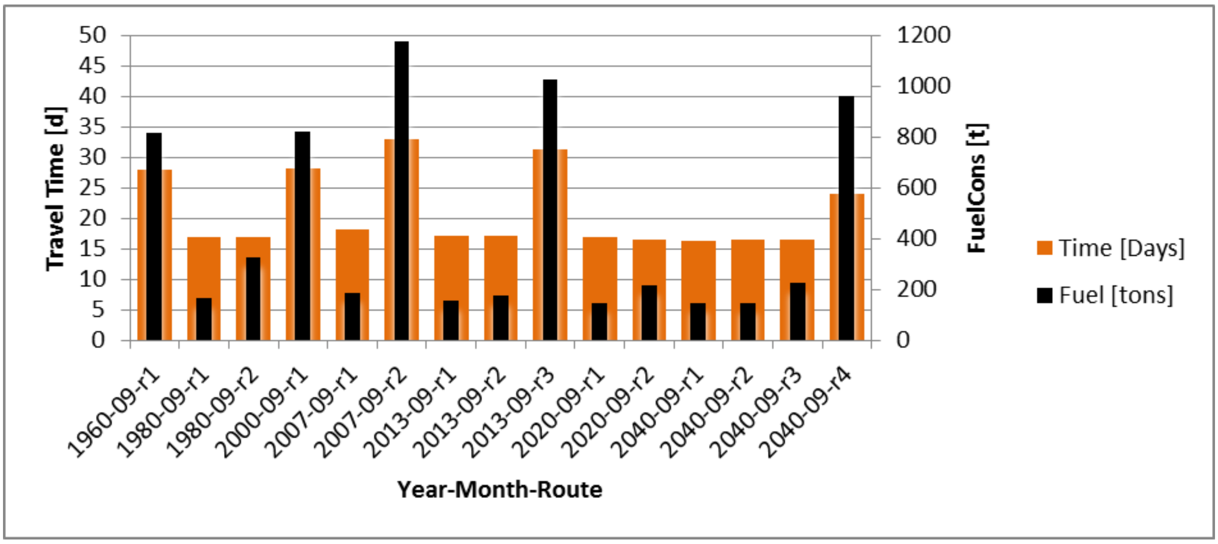

Figure 21 Tanker021, stating only completed transits

The longest travel time combined with the maximum fuel consumption is listed with 32 days and less than 1200 t of fuel. Weak regularities appear according to certain routes, that show a low success rate with route 4 and the highest quantity of completed transits on route 1. Shortest travel time is 16 days with 150 tons fuel consumption. The only month showing reasonable travelling time values for the tanker is September.

Tanker022

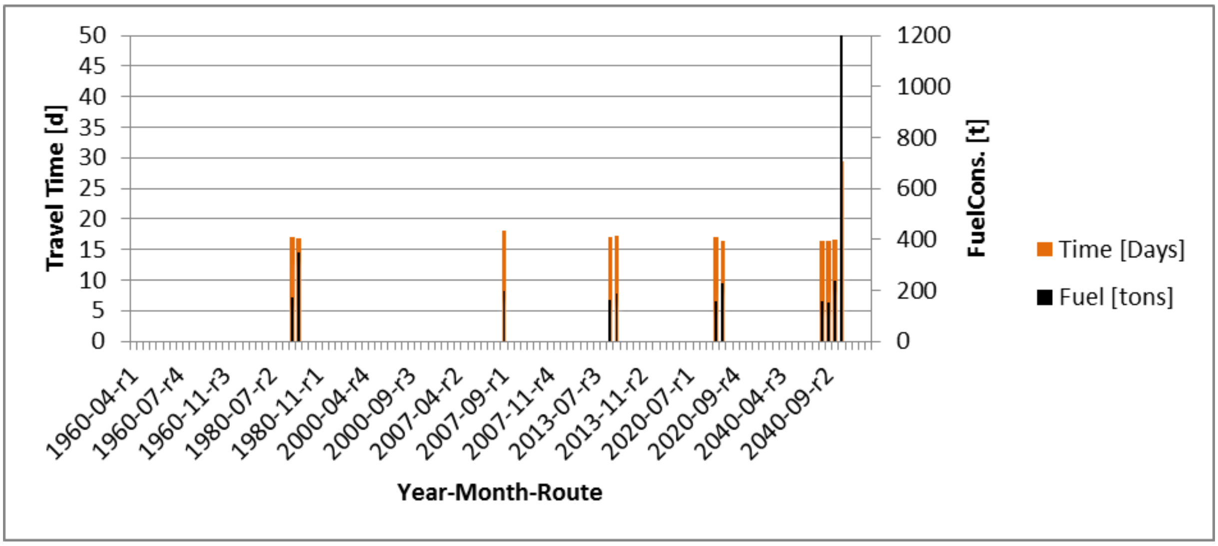

Figure 22 Tanker022 at all calculated routes

The most completed transits are registered with route 1. According to these calculations there will be possible completions of the routes 3 and 4 in 2040, even if route 4 shows the maximum time and fuel requirements. The travel time averages with 17 days. The only reasonable month for transits is again September.

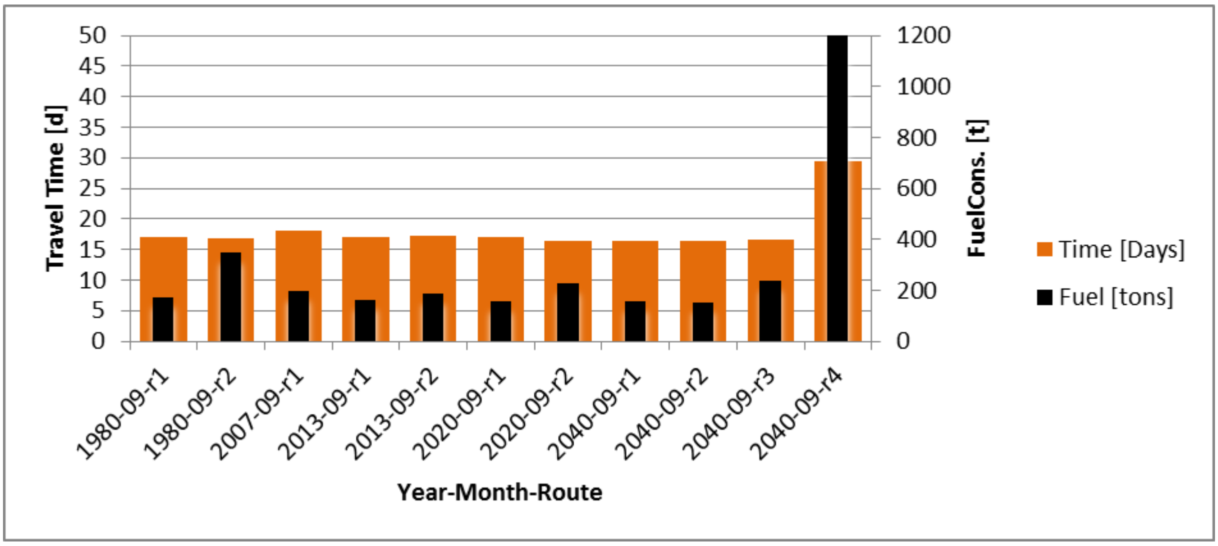

Figure 23 Tanker022, stating only completed transits

The longest travel time combined with the maximum fuel consumption is listed with 29 days and 1200 t of fuel.

Tanker023

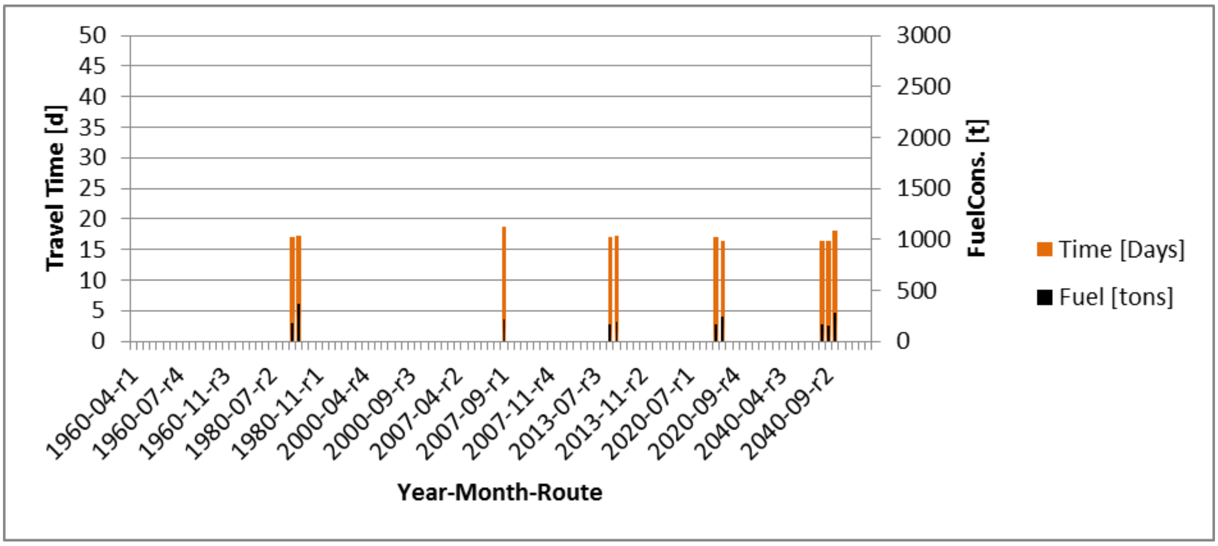

Figure 24 Tanker023 at all calculated routes

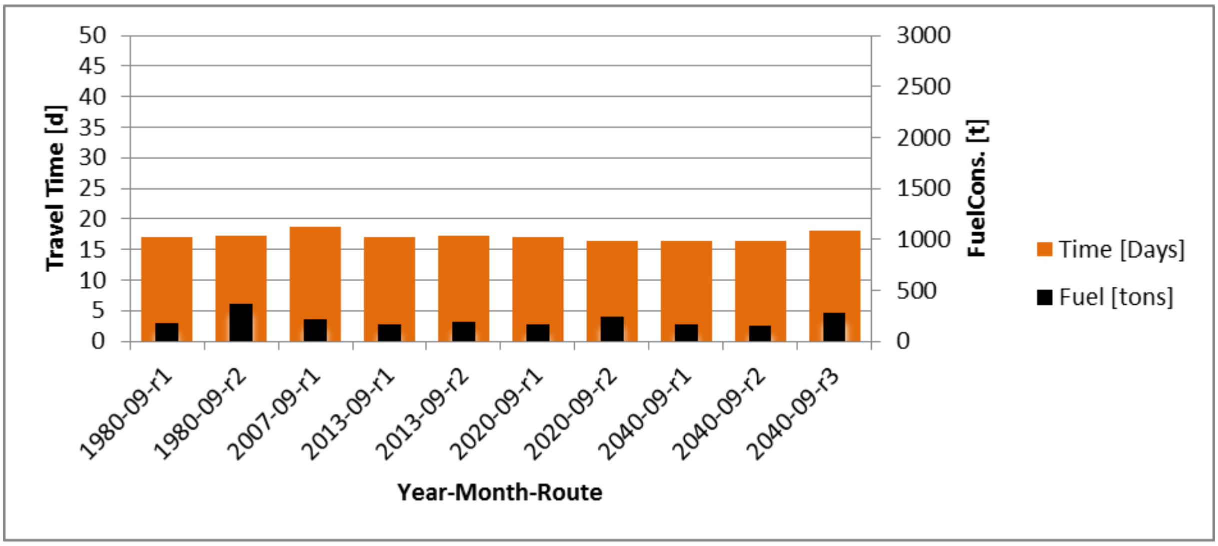

Figure 25 Tanker023, stating only completed transits

Figure 24 and Figure 25 again show the month September as only possibility to cross the routes. Mainly routes 1 and 2 are passed and with the assumed decreasing ice thickness route 3 will be passable.

From the first observed Tanker until here a slight decrease of fuel consumption is recognizable. In this case it averages at 200 t and develops no peaks. The travel time is stable on completed routes at 16 days, similar to the aforementioned Tankers.

There are only a few completed transits. The rate decreases slightly in comparison to the former Tankers as the pitch ratio is increased.

Bulker

The two bar charts in Figure 26 Figure 27 show the results for the bulker.

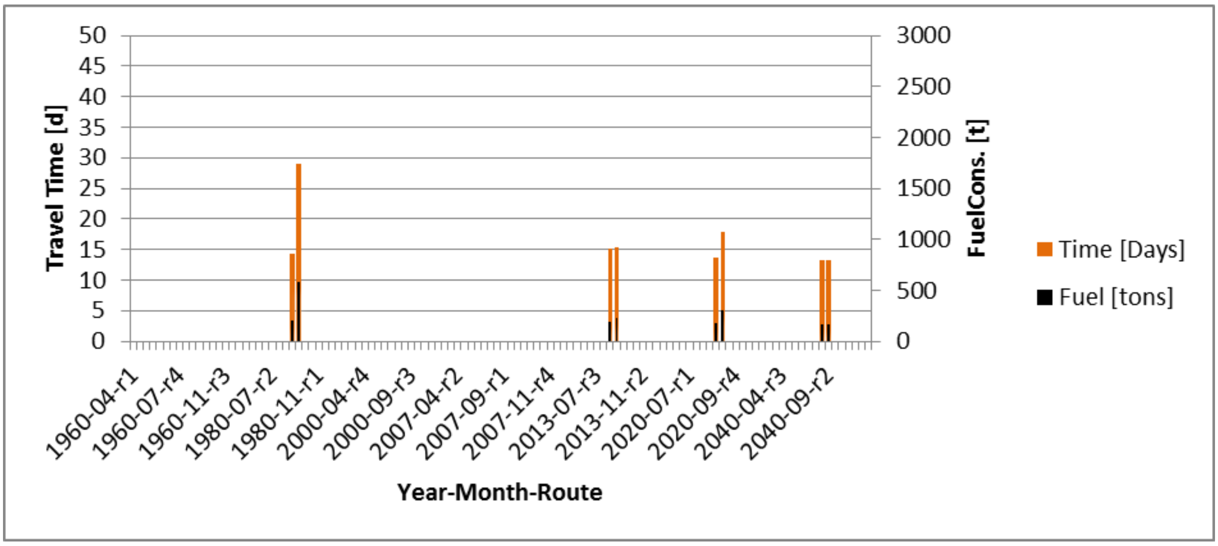

Figure 26 Bulker at all calculated routes

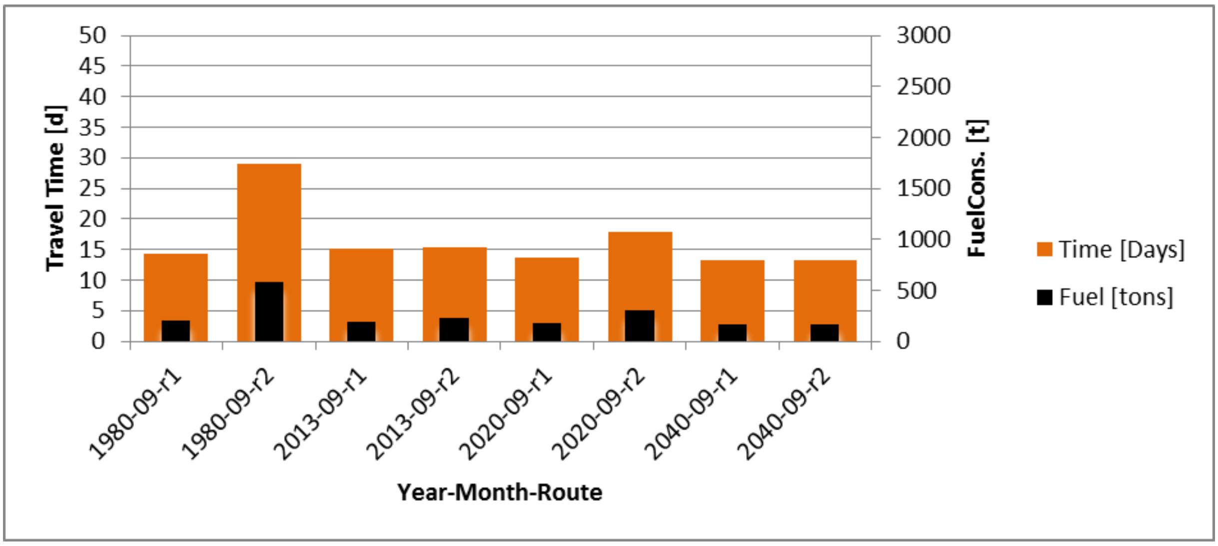

Figure 27 Bulker, stating only completed transits

There are very few completed transits. In particular the second figure shows the limited success rate. September is the month with the fewest ice thicknesses and concentration (c.f. section 3) and is in this case again the only period allowing the passing of the bulker.

The average consumption levels off at about 250 tons, the travel time at 14 days per completed transit. The fuel consumption stays moderate and does not exceed 600 t at the longest travel time of 29 days in total. Shortest travel time is in accordance with the calculations 13 days with 170 tons of fuel consumed.

LNG Carrier

The routes were calculated for two LNG Carriers. These ships differ in the engine power: the first one, delivering about 27 MW (l) and the second one, delivering 41 MW (h).

LNG Carrier (l)

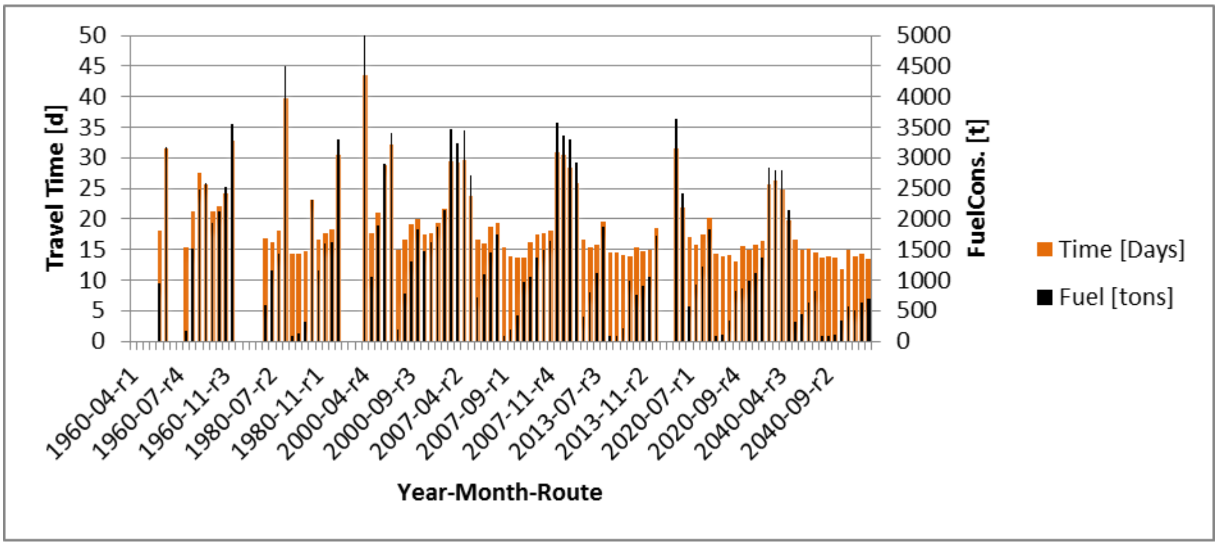

Figure 28 LNG Carrier (l) at all calculated routes

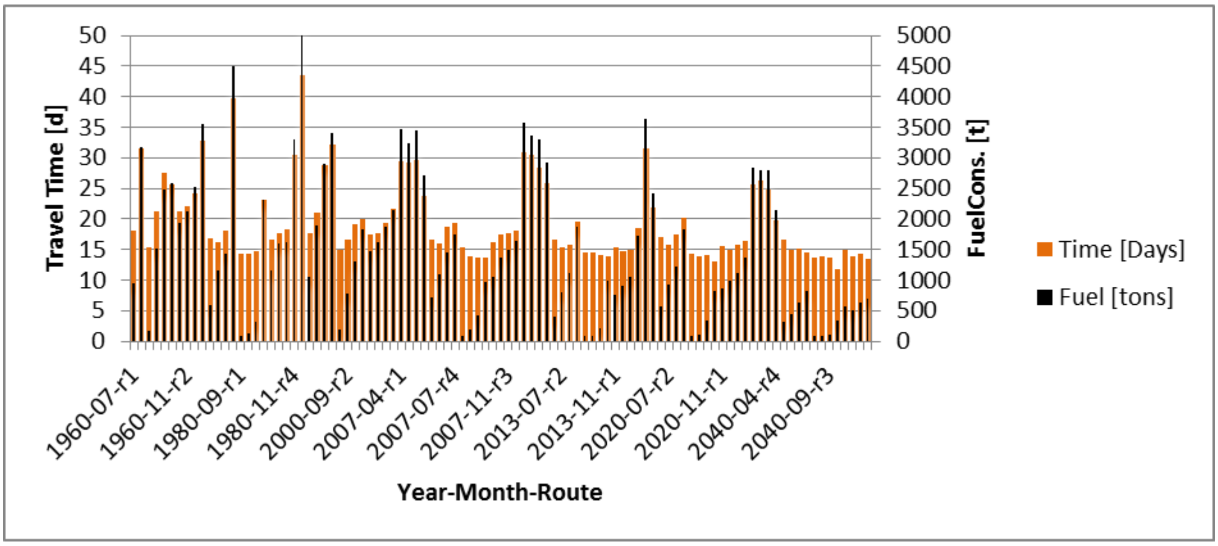

Figure 29 LNG Carrier (l), stating only completed transits

Due to its high ice breaking capability the LNG Carrier (l) shows a high rate of passing routes throughout from route 1 to 4. Main differences between the particular route calculations result from strong peaking in the fuel consumption. A few peaks reach values about 3500 t and more. Travelling times rise up to 30, detached up to 40 days in July and November.

Travelling times increase as the routes (e.g. 3 and 4) converge in the pole region and thus heavier ice conditions concerning thickness and concentration.

Within the scope of detailed views of the bar diagrams, as shown in Figure 30, it is recognizable that the fuel consumption from route 1 to 4 nearly rises linear with minimal values at route 1 and maximum at route 4. This trend is observable in Figure 28 and Figure 29 as well.

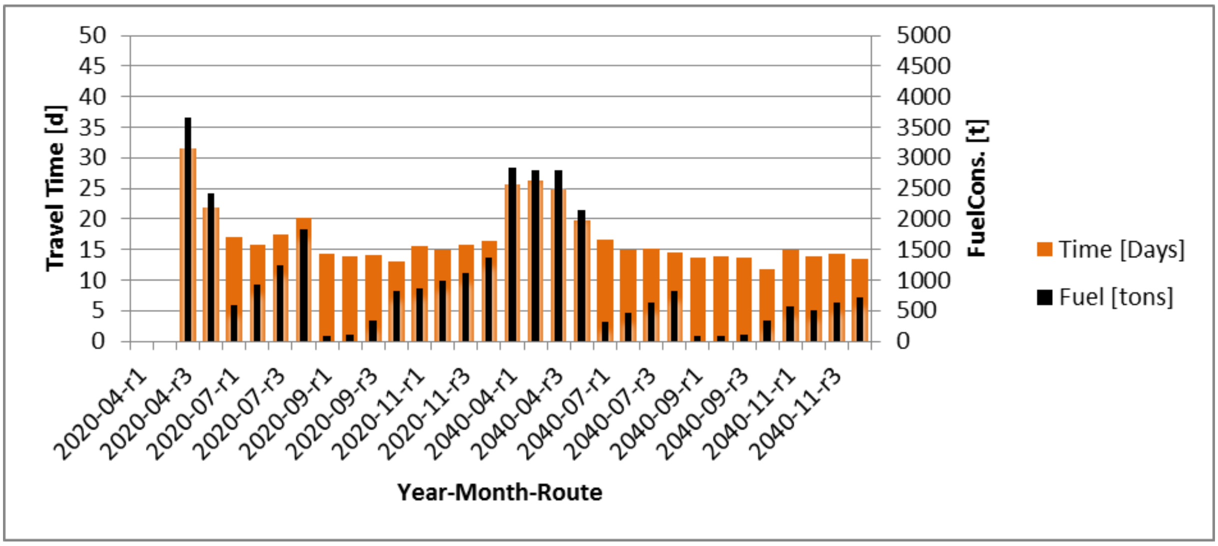

Figure 30 LNG Carrier (l), focus on years 2020 and 2040

LNG Carrier (h)

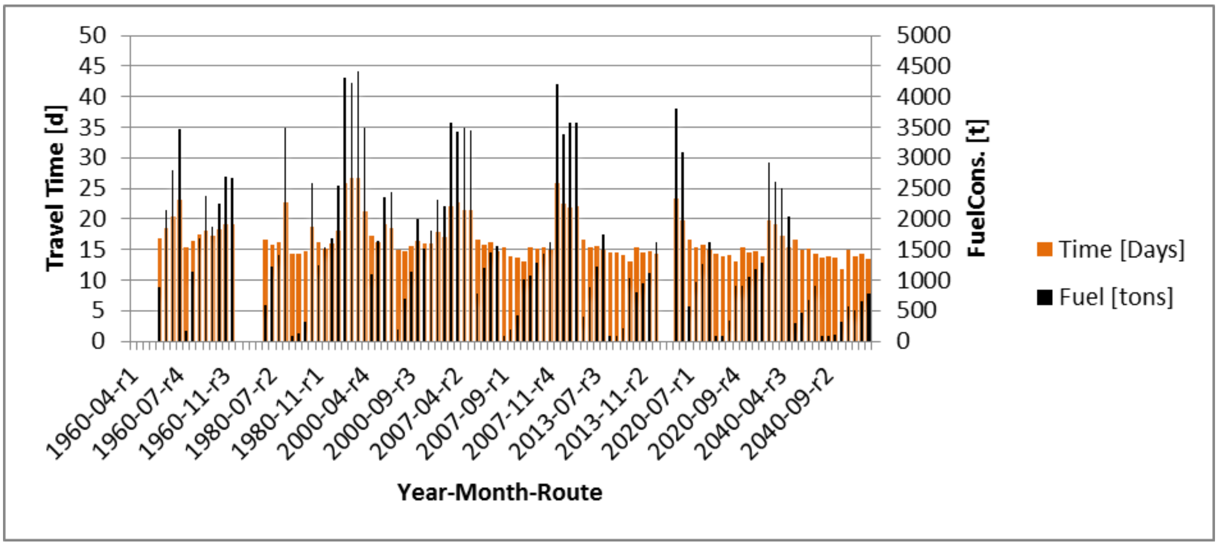

Figure 31 LNG Carrier (h) at all calculated routes

The LNG Carrier (h) shows, in resemblance to the LNG Carrier (l), a tremendous amount of fuel consumption. Especially route 3 and 4 in the periods of April seem hard to pass and stretch the travelling times up to 25 days. The average fuel consumption grows as a result from higher engine power. Remarkable are the very low consumption rates in the aforementioned month of September. In general there is a high resemblance between the two LNG Carriers.

Ice thicknesses of above 3m are defined as not finished as these conditions reflect unrealistic economic operational scenarios for icebrakers.

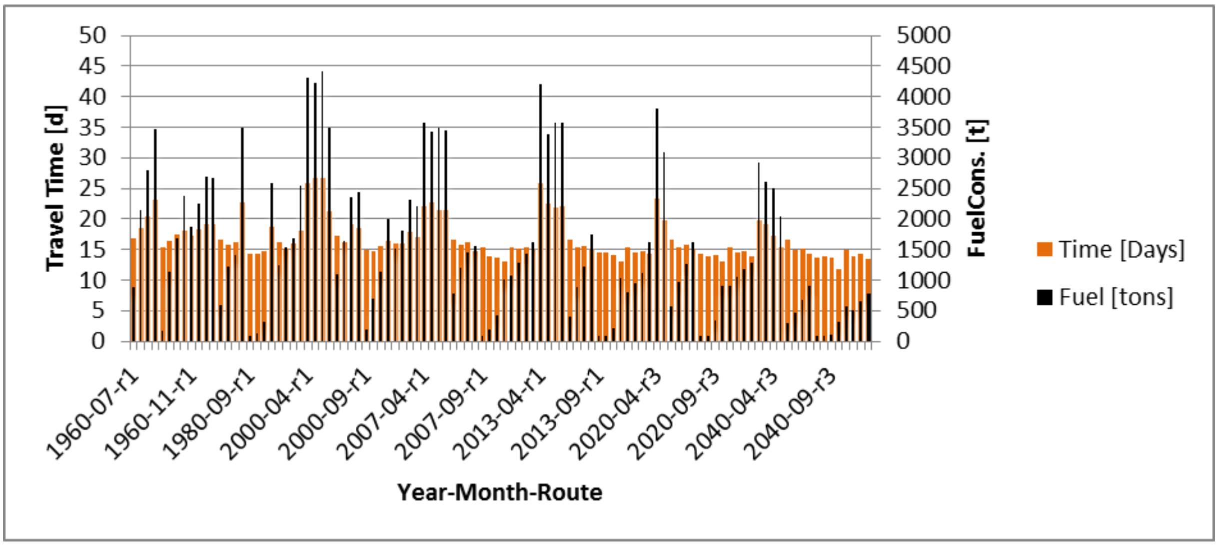

Figure 32 LNG Carrier (h), stating only completed transits

4.2 Exhaust gas emissions

For the environment especially the resulting emissions are of central importance. They are calculated proportionately to the fuel consumption, which will be enlisted with bars as well. A few noteworthy cases will be accentuated in the following passages.

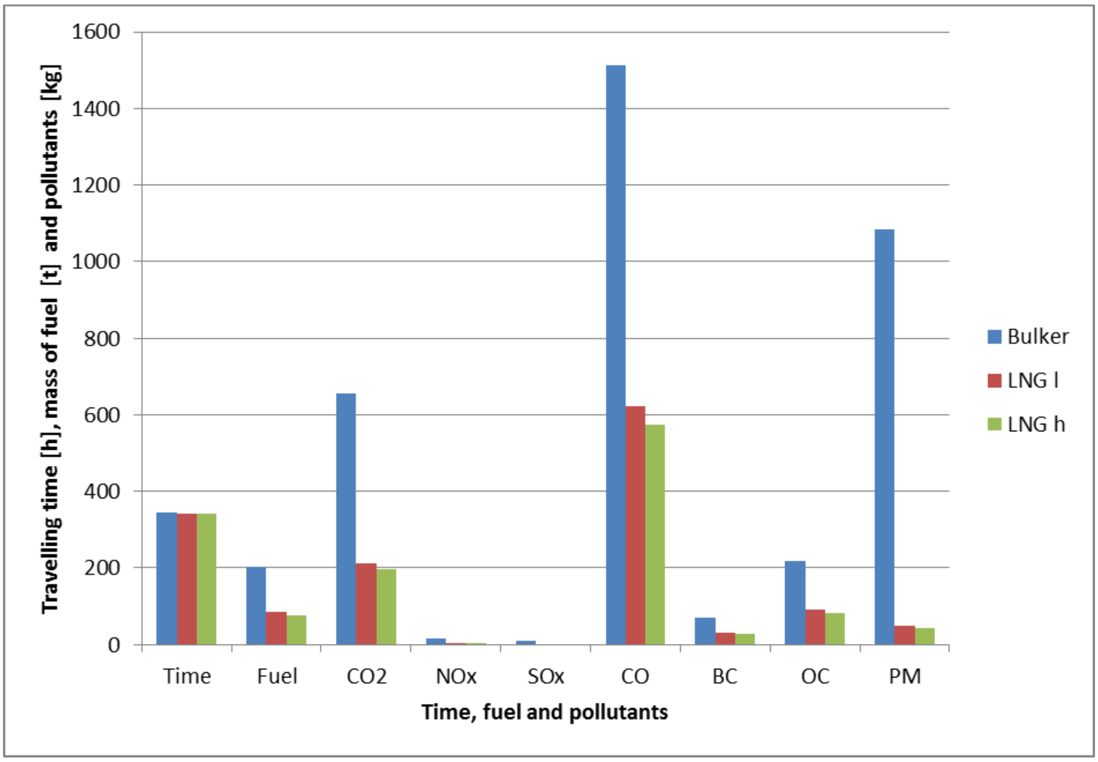

Figure 33 Exhaust gas emissions from LNG Carriers and the Bulker in [kg] (1980-09-r1)

For this consideration the 1980-November-Route 1 was chosen, as it was one of the only transits completed by every ship. Figure 33 shows a comparison of the LNG Carriers and the Bulker, concerning the exhaust gas emission data. The travel can be assumed as equal in the three shown cases. The figure shows that the Bulker needs more fuel and consequently exhausts more pollutants. Regarding the differences, it is important to point out, that the LNG Carriers do not exhaust SOx, because of the dual fuel propulsion concepts, whereas the two-stroke engines exhaust SOx. The Bulker exhaust approximately 15,9 kg of NOx and 11 kg of SOx. Mentioned values can be found as well in Figure 34 and state the maximum in these bars.

Figure 34 shows that the least emissions are exhausted by the Tanker01, which is again directly coupled with the fuel consumption. It is important to consider, that this route seems to be relatively ice free, as the ships have short travel times. This results in lower fuel rates, as the ships delivering less engine power are able to travel at a low power level due to the save speed in partly ice covered regions.

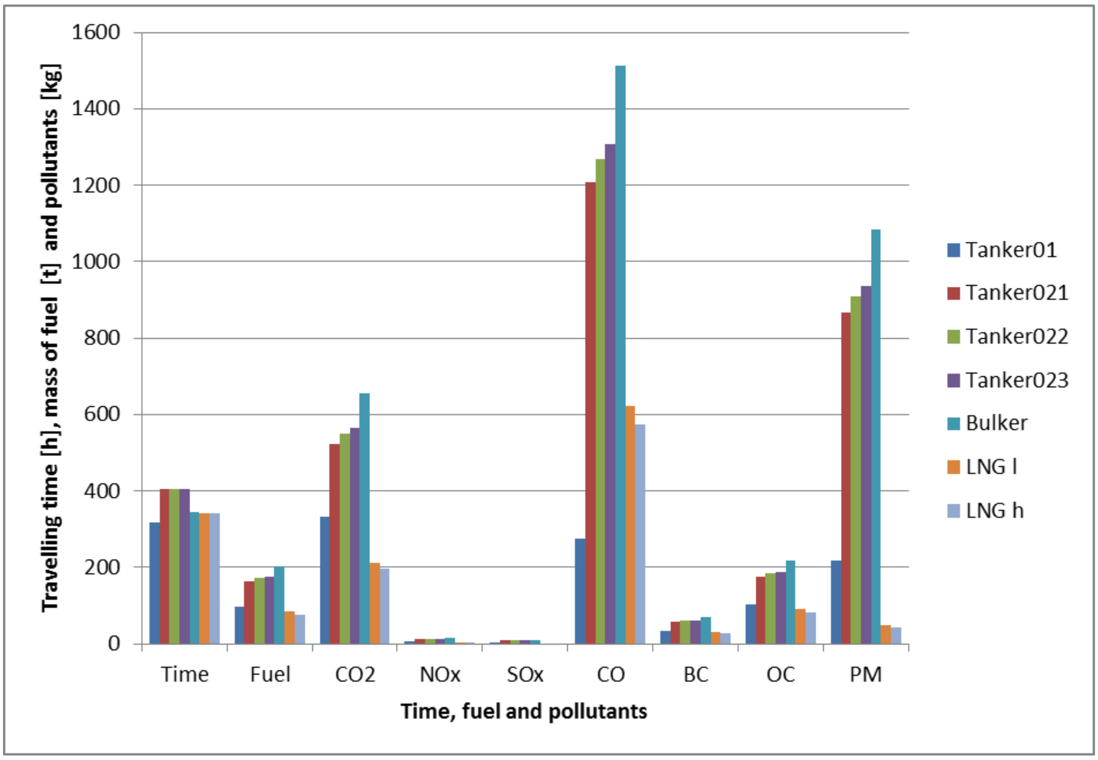

Figure 34 Exhaust gas emissions from all investigated ships in [kg] (1980-09-r1)

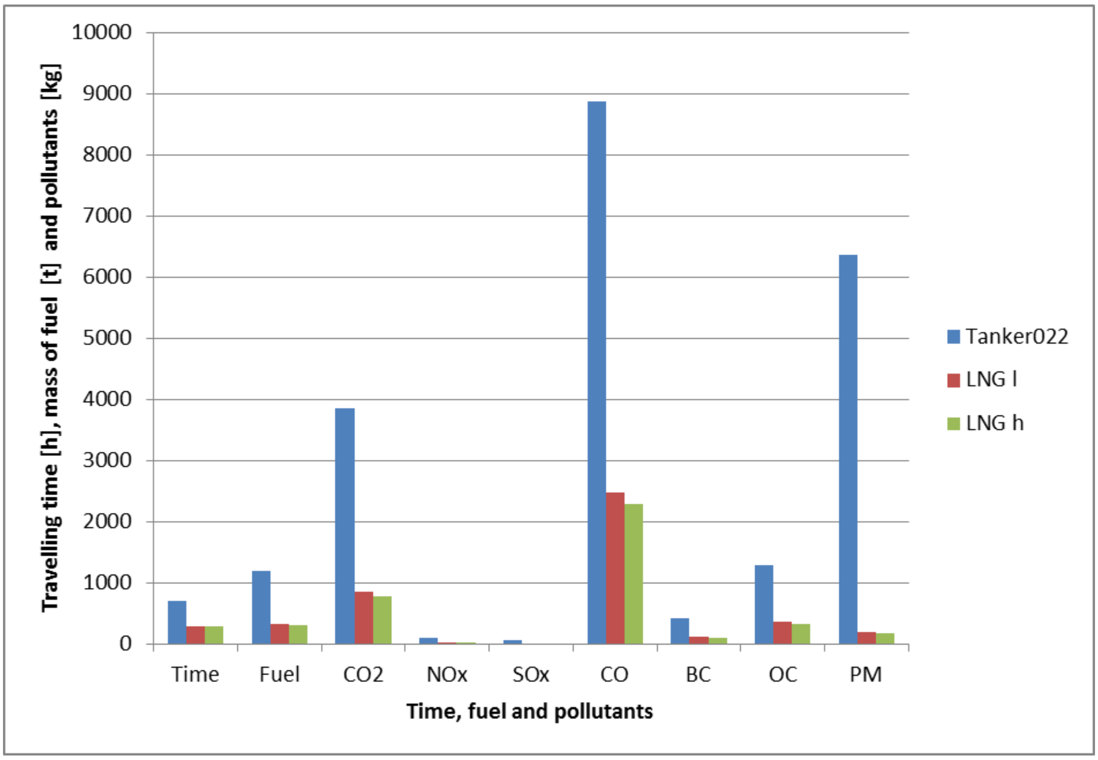

Figure 35 Exhaust gas emissions from LNG Carriers and the Bulker in [kg] (2040-09-r4)

Therefore another route will be highlighted: Figure 35 presents the emission data calculated for the Tanker01 and the two LNG Carriers. It is calculated for route 4, which is closest to the north pole and therefore covered with more ice throughout the whole year as shown in section 3. It is a forecast for November 2040. The results show that the Tanker01 has much higher consumption rate as the travel times is about 30 days compared to 11 days for the LNG Carriers. In this case obviously the emissions depend on the travelling time as stated before. The CO values have a peak at about nearly 9000 kg. The magnitude of the LNG Carrier’s emissions is about one third of the Tanker01’s.

Maximum values for the emissions values are in detail 93,6 kg of NOx and 64,6 kg of SOx. These are in this case exhausted from the Tanker01’s two-stroke engine.

As the result of the calculations directly depend on the fuel consumption, the exhaust gas emissions are better represented in the fuel consumption data.

5. Evaluation of the Fuel Consumption and Exhaust Gas Calculations

The presentation of the results stated, amongst travel time, the magnitude of fuel consumption and thus the exhaust gas emissions of different ships in arctic conditions. Dependencies on the routes 1 to 4 from coast to pole and on the seasons from April to November have been exposed.

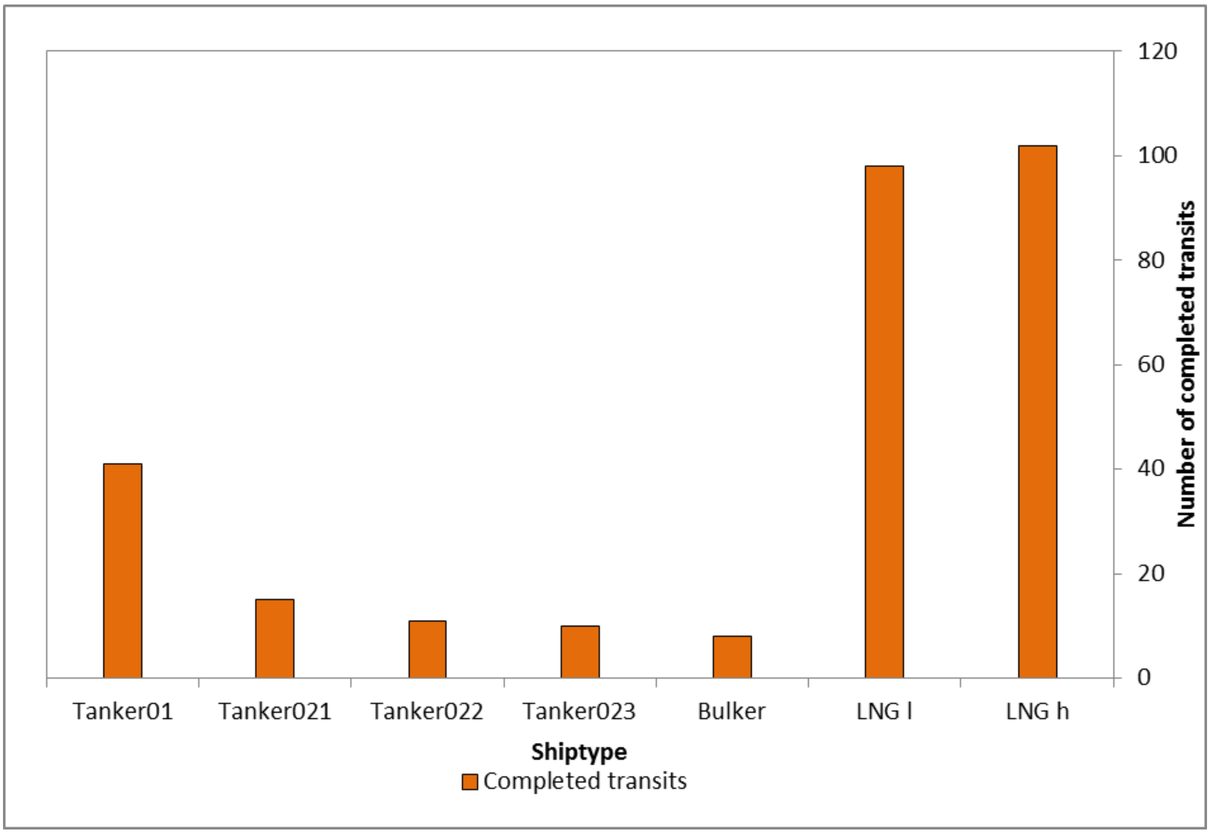

Figure 36 Overview of the total number of completed transits per ship

For the various Tankers and the Bulker very few completed transits have been calculated. These were limited to the months of September, where the ice conditions allow a safe passage. Furthermore they are coupled directly with the geographical circumstances of the routes, as shown in section 3.

The LNG Carrier in contrast shows a lot completed transits in both registered cases but with tremendous amounts of fuel consumption as the travel time in itself rises.

Figure 37 specifies the maximum delivered power of all investigated vessels, combined with their particular averaged fuel consumption per day. It indicates that the LNG Carrier (h) and (l) almost need the same averaged amount of fuel, whereas they both make about a 100 transits in total. Another reason for their high consumption is the ability of the LNG Carriers to make it through thick ice, as they deliver enough of engine power in combination with an extended ice breaking capability.

Taken into account the results shown in Figure 36 the comparison between the different tankers is to be pointed out. Whereas the Tankers 021 to 023 deliver the same power and differ from the angle of pitch, Tanker 023 needs the least amount of fuel. Here is to mention, that Tanker 023 also completes the least transits in total. This is realistic as Tanker 023 operates at an increased pitch angle which is optimal at situations is open water with low speeds. When the resistance is increased, the main engine is not able to deliver a sufficient torque moment at a small RPM. This makes it impossible to operate at low speeds with a high resistance.

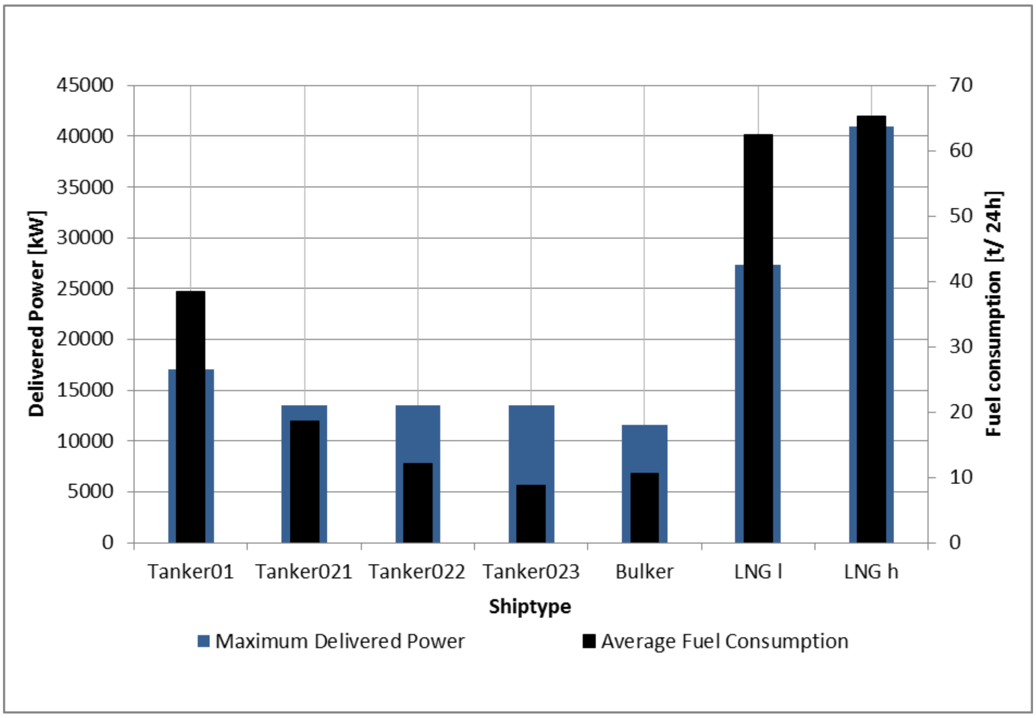

Figure 37 Overview of the maximum delivered power and the fuel consumption of 24 h

The results have clearly shown the consequences concerning time and fuel consumption resulting from taking the northern sea routes in months other than September. In addition it has made visible that the routes 3 and 4 are hard to pass in the present, since the results of the calculations show the first arguable completed transits in 2040.

6. Conclusions and Future Prospects

The results of the performed fuel and exhaust gas calculations show a clear trend of decreased travelling time for all ship types due to the decline of the arctic sea ice coverage and thickness. This is coupled with lower fuel consumption rates and consequently lower exhaust gas emissions of ships. On the other hand it is possible for more vessels even with a low ice breaking capability to cross the NSR. Thereby the total amount of exhaust gases may be raised especially when ships operate at the maximum available main engine power for a longer time.

Advantageous is, that when the ships are traveling at a save speed in regions with a small ice coverage, the fuel consumption is quite low. The speed has to be limited in ice covered regions to avoid damages by ice contact. Due to that the ships traveling time is not significantly increased when the ice conditions get worse. By the restriction to safe speed of for example 8 knots slow steaming scenarios are obtained which might lead to lower fuel consumption / exhaust emission compared to conventional routes to far east.

It was further shown, that traveling on several routes, e.g. on route 2, in certain periods other than September, increases the fuel consumption rapidly. Using this new developed tool certain scenarios can be easily simulated and compared. Thereby the influence of the arctic shipping on the NSR regarding the environmental pollution can be calculated.

The future forecasts denote a widening of operation windows for transits on all routes and especially in the freeze up periods of October and November. To predict future scenarios the ice forecast is the main uncertainty of the calculations.

This report focuses on the exhaust gas emissions and the evaluation of the program for the calculation. It was shown what coarse magnitudes of emissions vitiate the sensitive polar region, caused by ship transits.

To summarize, it must be stated that there is no unambiguous relation between ice situation (extent, thickness, coverage) and the fuel consumption and exhaust emission. The reason is that if the ice extent increases towards the winter period less ships are able to travel the northern routes in a reasonable time. Additionally in the intermediate periods (freeze up and melting) ships will be restricted in speed due to safety reasons. In order to accumulate exhausts emissions for the arctic region for future times the number of ships, which may operate under reasonable safe and economic conditions, has to be determined. This number will be depending on the development of the region and its infrastructure (socio economic factors). Additionally the travel time and operation condition of the different ship types will be of major concern as the speed profile will not only depend on technical ability but on freight rates and type of goods to be transported along the Northern Sea Route.

For future prospects, with more accurate classification of emission factors for certain propulsion arrangement, a fairly adequate assessment of emissions can be reached

References

[1] ACCESS, „Final Proposal "Arctic Climate Change, Economy and Society ",“ 2011.

[2] HSVA, „Final public report on the ARCDEV project,“ EU funded Project ARCDEV, 1999.

[3] Q.-T. Duong, „Calculation of Fuel Consumption and Exhaust Emissions from Ship in Ice Conditions,“ West Pomeranian University of Technology, Szczecin, 2013.

[4] HSVA, „D2.16 – Report presenting results of ICEROUTE calculations of traveling time for different scenarios and routes on NSR and NWSR in past, present, and future,“ Seventh Framework Programme, 2011.

[5] Wikipedia, „Brake specific fuel consumption,“ http://en.wikipedia.org/wiki/Brake_specific_fuel_consumption, webpage retrieved 10 May 2014.

[6] T. K. L. K. P. Borkowski, Assessment of ship's engine effective power fuel consumption and emission using the vessel speed, Journal of KONES Powertrain and Transport, Vol. 18, No. 2, pages 31-39, 2011.

[7] M. D. &. Turbo, „Exhaust gas emission control today and tomorrow – Application on MAN B&W two-stroke marine diesel engines,“ Technical paper, 2009.

[8] M. D. &. Turbo, „Emission control two-stroke low-speed diesel engines,“ Technical paper, 2009.

[9] J. J. L. D. A. W. J. J. H. S. S. J. A. G. M. Corbett, Arctic shipping emissions inventories and future scenarios, Atmospheric Chemistry and Physics, 2010.

[10] Notz, D., F. A. Haumann, H. Haak, J. H. Jungclaus, and J. Marotzke (2013), Arctic sea-ice evolution as modeled Max Planck Institute for meteorology's Earth system model, J. Adv. Model. Earth Syst. 5, 173–194, doi:10.1002/jame.20016.

[11] Karl E. Taylor, Ronald J. Stouffer, and Gerald A. Meehl, 2012: An Overview of CMIP5 and the Experiment Design. *Bull. Amer. Meteor. Soc.*, **93**, 485–498. doi: http://dx.doi.org/10.1175/BAMS-D-11-00094.1

[12] Riemann-Campe, K., Arctic Sea-ice in Climate Scenarios, personal Communication, Powerpoint Presentation, ACCESS, 2013, https://wiki.met.no/_media/access/ga/2014-03/2014_ga_wp1_summary.pdf

[13] Richard H. Moss[1], Jae A. Edmonds[1], Kathy A. Hibbard[2], Martin R. Manning[3], Steven K. Rose[4], Detlef P. van Vuuren[5], Timothy R. Carter[6], Seita Emori[7], Mikiko Kainuma[7], Tom Kram[5], Gerald A. Meehl[2], John F. B. Mitchell[8], Nebojsa Nakicenovic[9,10], Keywan Riahi[9], Steven J. Smith[1], Ronald J. Stouffer[11], Allison M. Thomson[1], John P. Weyant[12] & Thomas J. Wilbanks[13] The next generation of scenarios for climate change research and assessment , *Nature* **463**, 747-756 (11 February 2010) | doi:10.1038/nature08823